POLITECNICO DI TORINO

Dipartimento di Meccanica e Aerospaziale (DIMEAS)

Master's Degree in Automotive Engineering

Master's Degree Thesis

Design and simulation of a Battery Swapping System for public transport

Supervisors:

Prof. Giulia Bruno

Prof. Franco Lombardi

Dott. Alberto Faveto

Author:

Utkucan KARADUMAN

February 2021

Acknowledgment

I would like to express my special thanks of gratitude to my supervisor Prof. Giulia Bruno as well as Dott. Alberto Faveto for giving me the opportunity to make research on this interesting subject and for providing guidance and help throughout this research.

I am also thankful to all my friends who shared their supports with me all the time. Seren, Nogay, Musa, and Togrul are the ones who deserve a special thanks for being always there for me.

Lastly, I would like to acknowledge with gratitude, the support, and love of my family.

Abstract

Nowadays, the automotive industry faces one of the biggest transformations ever. As the concerns about greenhouse gas emissions and global crude oil demand grow, the automotive industry undergoes a change towards the use of electric vehicles (EVs) over traditional internal combustion engine vehicles. For a greater revolution, EVs need to point out issues such as long charging times, insufficient charging infrastructure, low battery performance, high price, fleet electrification, as well as powering renewable energy-based charging grids. As a result of these problems, vehicle manufacturers have started to investigate and invest in more cost-efficient and innovative solutions to engage with the issues related to using electric vehicles. For instance, in order to overcome the long battery charging times, the battery swapping systems (BSS) have been introduced. BSS can be described as the service station in which depleted batteries can be exchanged with fully charged batteries in a fast and functional way without experiencing the waiting times. The recharge of the battery will then be carried out at a later time.

The thesis discusses the design and simulation of a BSS solution for public transport, in order to evaluate the potentiality of its application. As a case study, the simulation model is built with respect to the buses operating in the city of Turin. Therefore, the characteristics of batteries and the number of buses circulating are selected appropriately. Several experiments are executed through FlexSim, a 3D simulation modeling and analysis software, to obtain the adequate size of the battery swapping station for retaining the desired public transportation services and to find out which factors can cause the station to underperform. The most suitable solution is chosen through a multiple-criteria decision analysis (MCDA).

Contents

List of Figures

List of Tables

1 Introduction

The thesis aims to design an automated battery swapping station for electric buses by implementing its model into a simulation environment to better control and track the performance parameters. The outcomes of the thesis will provide a feasibility analysis and a design solution for the governments and municipal corporations which have intentions to invest in this subject.

The thesis is comprised of five chapters and it is structured as follows.

Chapter 1: deals with the definition of the battery swapping station and exposes the positive and negative characteristics of it by making a comparison with conventional battery charging systems. It also explains the charging rules of the electric vehicles and specifies the distinctive features of batteries of the leading electric bus manufacturers.

Chapter 2: provides recent techniques adopted for battery swapping system for public transportation and explains the battery exchanging mechanism.

Chapter 3: states the assumptions that are conducted during the model definition and how the simulation model is built to design an automated battery swap station with regard to data which are obtained by analyzing the public transportation of Turin.

Chapter 4: comes up with the results of the simulations that have been performed by considering different scenarios and highlights the best fitting case in terms of performance and cost-effectiveness.

Chapter 5: proposes sights to improve the established model of designated swapping stations and future concepts and ideas for further improvements.

1.1 E-mobility in Public Transportation

A recent study carried out by the University of Oxford demonstrates the global greenhouse gas emissions produced by each sector in 2020. One of the non-negligible figures has appeared as the transport sector with 16.2% and it does not even take into account the emissions from the manufacturing of motor vehicles or other transport equipment. Road transport with 11.9% is the major factor of emissions which is caused by the burning of diesel and petrol from all type of road transport which includes cars, buses, motorcycles, lorries, and trucks.[1] It can be pointed out that electrification of the all-road transport sector feasibly decreases global emissions by 11.9%.

Taken as the basis of similar researches with increasing concerns about dependency on petroleum and the developments in battery pack technologies and electric powertrains, many governments and automotive OEMs across the world have increased the attention on eco-friendly vehicles. Therefore, the rise of the popularity of electric transport was inevitable since expanded electrified public transport had crucial importance to address the issues such as the rise in pollution, environmental hazards, and stringent government regulations. As a result, electric buses have achieved a significant growth rate in the market. The global electric bus market, by volume, is estimated to be 136,537 units in 2019. It is projected to grow at a compound annual growth rate of 27.2% to reach 934,717 units by 2027.[2]

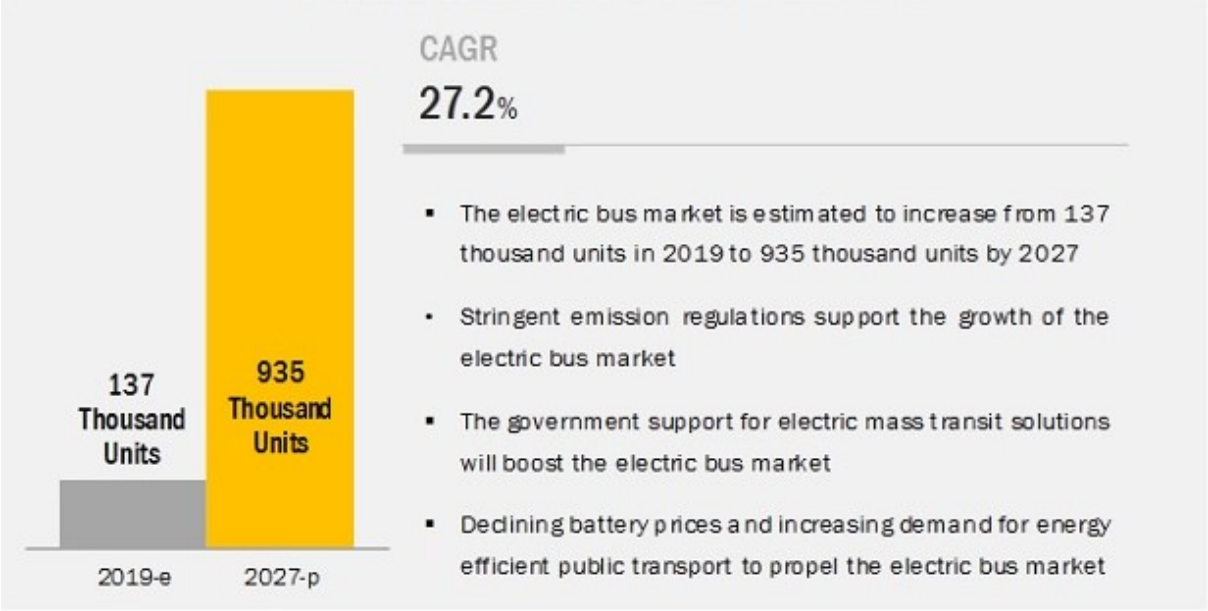

Figure 1.1: Attractive opportunities in the electric bus market [3]

Another research carried out by Statista represents the total number of electric bus fleets with respect to the regions and countries. A similar growing trend in the electric bus market can be observed, and registrations of electric bus fleets are expected to triple in 20 years, rising from 400,000 units to 1,200,000 units. Asia-Pacific region has been leading the electric bus market, with increased governmental initiatives in countries such as China, Japan, and India. In the current situation, particularly, China is the most encouraging market in this sector such that in 2018, 23% of the purchased buses were electric, and it is expected to lead the demand for e-bus over the forecast period with more than 400,000 new purchases by 2025. The US and Europe are prominent markets likely to follow the Chinese e-bus market. In 2019, the registrations of new electric buses in the European region increased by 170.5% from 594 units in 2018 to 1,607 buses in 2019, and the expected contribution of these two markets will be more than 40,000 electric heavy-duty vehicles on the roads by 2025. The increment in the acquisition of electric buses is expected to rise as a result of government initiatives that support e-mobility consistently, and 40% of the purchases of buses are anticipated to be e-bus by 2040 on a worldwide scale. [4]

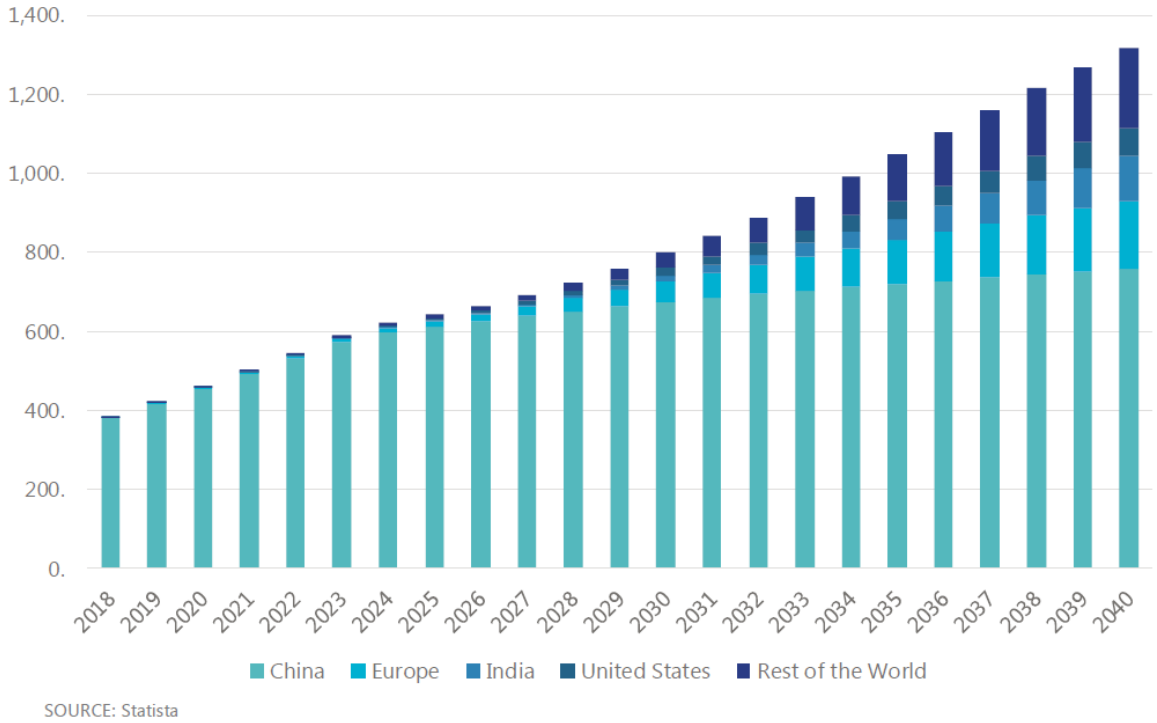

Figure 1.2: Projected municipal e-bus fleet in thousand unit, by region and country, 2018-2040 [4]

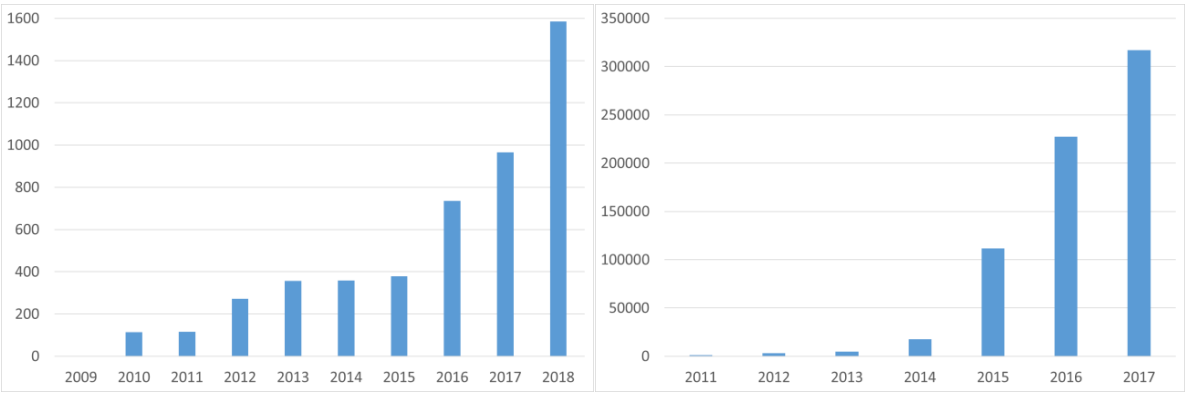

(a) (b)

Figure 1.3: EBs fleet(a) in Europe and (b) in China [5]

Figure 1.3 reveals again the rise of electric vehicles for public transportation in Europe and China respectively. China is again a leading country when it comes to the adoption of different techniques to charge EV's battery packs and battery swapping stations are in service in addition to wired and inductive charging. According to the annual report of the State Grid

Corporation of China (SGCC),1.537 battery charging/swap stations have been constructed by December 2015 in China.[6]

The country's major EV manufacturer Beijing Automotive Industry Holding Co. Ltd (BAIC) provides battery swapping services dedicated to electric taxis. By the end of 2022, the installation of 3,000 battery swapping stations that can serve 500,000 EVs is planned by BAIC with a total investment of over $1.4 billion. [7]

1.2 Functioning of Battery Swapping Station and its Configuration

Battery swapping can be understood as the replacement of the used battery with partially or fully charged ones whose state of charge (SoC) level is depleted below its predetermined level to maintain the electrified transportation. The operating principle of BSS is FIFO (First in First Out) in which the vehicle arriving first gets the swapping service earlier compared to those who arrive later. To ensure the swapping operation for all the vehicles approaching the swapping stations, it is necessary that the batteries must be changed quickly in order not to cause the formation of a queue and that's why it is crucial to establish continuous communication between the station and the vehicles. In doing so, the driver can make the request for a battery swapping service prior to his/her arrival, and information regarding the location of the vehicle, its expected arrival time, and the battery type can be received by the station so that the station prepares the requested battery type by the time the vehicle arrives to station. The robotic arms are utilized to replace the discharged battery from vehicles with a compatible charged battery and to place discharged ones within the charging racks where slow and/or fast charging is taking place. Once the swapping operation is performed, the vehicle's battery will be analyzed immediately and the driver will be informed about its remaining charge, battery age, the number of charging and undergone discharging cycles, state of charge, state of health (SOH), and battery life.

The configuration of a BSS has also significant importance to manage with the fleet and to keep the duration of swapping operation in order of few minutes and that's why the elements that are employed in BSS such as the number of chargers, batteries, employees are decided in advance. Figure 1.5 shows one of the typical configurations of a Battery Swapping Station and it demonstrates the main components of a BSS such as battery chargers, AC-DC converters, robotic arms, distribution transformers, maintenance systems, control systems, and vehicle batteries. The distribution transformer has the role to receive the voltage from the grid power system which is between 11kV and 33kV and then it converts to the charger's nominal voltage that can be 120V/15A,240V/80A, or 50 kW and more. Battery chargers recharge the depleted batteries by utilizing the DC power that can be received by the application of the AC-DC converters (figure1.4). There are two possible ways to locate AC-DC converters. In the first configuration, one may have a centralized converter directly connected to the distribution transformer, delivering DC power to all the chargers. In the second configuration, all the charges take advantage of converters placed locally. The latter one is favored since it gives the possibility to carry on the operation when one of the chargers shows malfunctioning and also centralized AC-DC converters introduce drawbacks in terms of cost, weight, and size. BSS is also equipped with the battery management system called the Battery Energy Control Module (BECM) that has the role to monitor the voltage and temperature of each individual cell as well as the charging power of battery cells. It also controls the desired temperature of the battery cell and stabilizes the charging and the voltage across all of the cells of each battery pack.

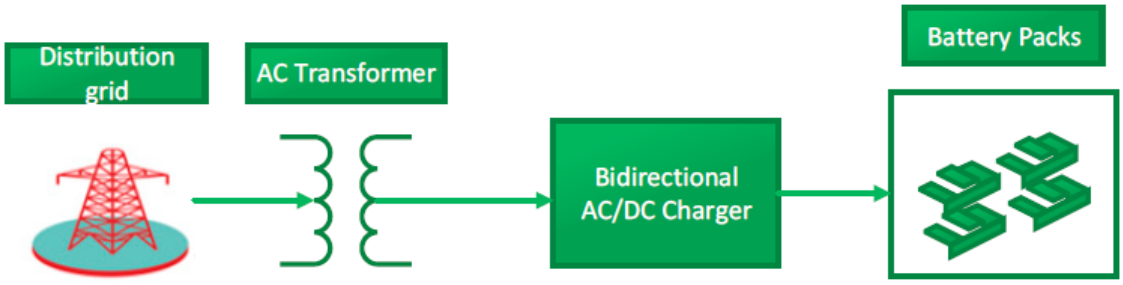

Figure 1.4: Block diagram of BSS electrical design [8]

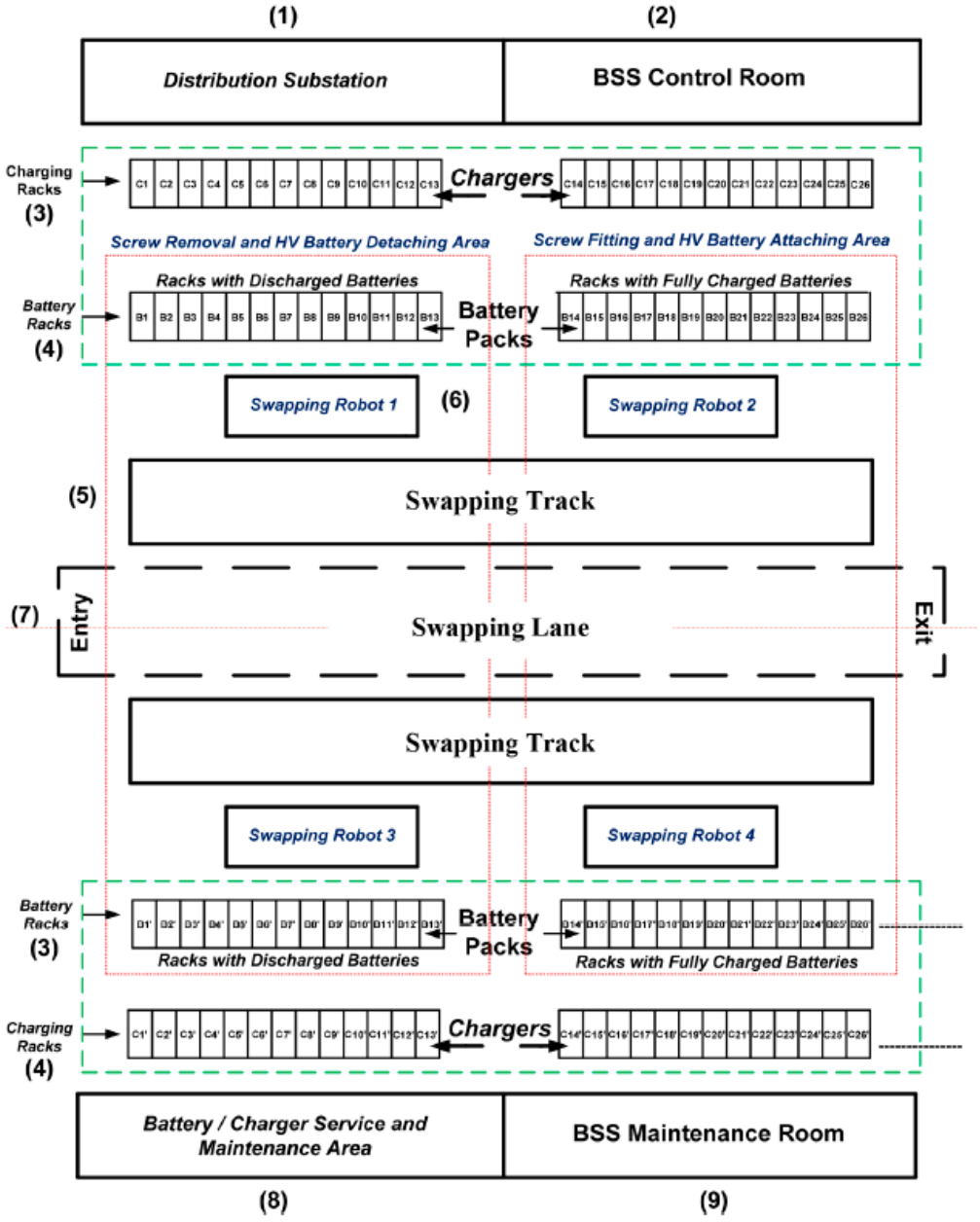

Figure 1.5: Typical configuration of a BSS [9]

According to the application point of the robotic arm for swapping operations and the position of the battery, it is possible to distinguish different battery swapping techniques without altering the general configuration of BSS and are given as follows:

Sideways swapping: Commonly used for vans and vehicles that have permitting sideways position.

Rear swapping: Usually employed for vehicles in which the battery is located at the rear end with large boot space.

Bottom swapping: Utilized for the vehicles whose battery is located at the bottom of the vehicle and it requires the positioning of the vehicles on an elevated platform and the batteries are swapped from the bottom using a robotic arm.

Top swapping: Generally used for the electric buses whose batteries can be found at the top and robotic arm can exchange the depleted batteries from the opening of the rooftop.

1.3 Adoption of Battery Swapping Station: Opportunities and Challenges

Charging EV battery can be done by different techniques that require particular charging equipment and infrastructures and there are three types of charging technologies available:

EV Battery Swapping System = The operation mode of the battery swapping system can be explained as the drivers simply drive their vehicles into the service area located in the battery swap station, align battery pack appropriately to avoid any damage, ensure the vehicle is completely immobilized during the process and battery pack is properly mechanically and electrically isolated. Firstly, the depleted battery is disconnected from the vehicle, and it is placed in the warehouse for charging, then a fully charged one is installed on the vehicle. The operations performed in BSS are under the control of a high level of autonomy.

Inductive Charging (Wireless Charging) = Charging station is able to supply power through the induction principle without requiring any physical contact between EV battery and EVSE. The electromagnetic field makes possible the energy exchange, and it is generated by an induction coil that is embedded in the charging station. A second receiving induction coil located inside

the vehicle is used to convert the power from the electromagnetic field into electrical current to charge the on-board battery.

Conductive Charging (Wired Charging) = Flow of power is sustained between EV battery and EV supply equipment (EVSE) at the charging station with the help of a physical connection that is called the conductive link. Conductive charging stations can be either AC- or DC-based. Since EV battery packs can only be charged with DC, for the case of the AC charging station that can be named as low power charging systems, conversion of AC from distribution lines into DC must be performed by the on-board battery charger. Whereas, in DC charging stations, direct current is sent directly to vehicle battery without passing through on-board charger and it is classified as the off-board charger.

Regardless of the fact that the battery swapping solution has not achieved success commercially and globally, it still stands as a viable and promising alternative over conductive and inductive charging for today's technology since it suggests extensive benefits and opportunities as against conventional charging techniques. One of the main benefits appertaining to battery swapping is that it resolves the issue of the battery charging speed. Unlike dedicated charging, it enables battery recharging to be completed in a few minutes which makes it as fast as refueling a gasoline-powered vehicle and eventually reduces the driver waiting time. Another benefit of the employment of the battery swapping is enhanced battery life and quality. When the battery is charged with the fast charging scheme (100 kW and more), battery degradation and sequential damages are inevitable. A battery that exhibits a prolonged life cycle and consistent power can be achieved by using BSS because it maintains an improved control strategy for charging, which is essentially charging at the required voltage for a longer duration and keeps the battery capacity and performance at the desired level. Bidirectional power flow between BSS and grid is another plus point. Apart from the fact that BSS supplies the power that is taken from the grid to charge batteries, it can turn back the power that is stored in batteries into the grid. BSS can make a profit and cut down the electricity cost by scheduling the charging times during off-peak hours that is characterized by

low demand (price) and by dispatching the stored power in the batteries into the grid during peak hours which displays high demand (high price). Meanwhile, the reliability of the power grid is improved with the mentioned charging /supplying patterns as a result that overloading to the power grid that may be generated by excessive charging loads are reduced. Additionally, BSS can provide more services to return more profit and these services could be frequency regulation, regulation reserves, voltage support, demand response, and energy arbitrage. [8-9] By the adoption of BSS, another advantage can be gained from the customer perspective. One of the major barriers to hinder the widespread adoption of electric vehicles from the customer's point of view is the high cost of ownership of EVs and consequently highly related to the cost of the battery, which is equivalent to 25 to 50 % of the total cost of the EV. BSS plays an important role in reducing the high price of EVs as it offers to hold the ownership of the batteries and it suggests a leasing model. In this model, BSS is in charge to monitor the health of the batteries and making the replacement with the new ones as they approach the end of their lifecycle. Furthermore, continuous improvements in charging technology impose EV users and other charging stations to upgrade their charging equipment to benefit from the latest technology. In this respect, upgrading the BSS is much more efficient and easier than upgrading a vast number of charging stations located in different locations or at household levels.

Even though the adoption of BSS promises several benefits and opportunities, there are also some challenges and drawbacks associated with BSS that must be addressed and be overcame. One of the main hindrances that restrain the spread of battery swapping technique is the lack of standardization of battery packs. One can find distinctive battery architectures manufactured by OEMs, and it is not feasible nor possible to hold all of them in the inventory of BSS which obliges the swapping station to operate with the limited number of battery types. To resolve such a challenge and to maximize standardization, interchangeability between different battery packs must be achieved by means of brand compatibility and cross-platform but such approaches have some risks that may result in singularity, non-innovative, and non-flexible product development [9]. The other difficulty that battery swapping technology currently encounters is the battery pack design. To remove and reattach the battery packs quickly and effortlessly, they have to be designed in a particular way and they must be located in positions that are easily accessible by swapping robots. An initial investment of building the

BSS can be regarded as another roadblock that still stands in front of it. Comparing to conventional charging stations, the infrastructure of BSS requires more investment to start operating. These additional expenses are needed for setting up the automated swapping platform, acquisition of batteries that fulfill the daily requirement, equipment used for internal logistic activities, and warehousing structure. There are also some concerns from the customer's point of view. Low energy storage of the batteries due to degradation over time is certain and therefore, the customer will have a tendency to prefer the latest battery packs more than the option of other relatively old battery packs as they offer a wider range and minimize the number of trips to the swapping station. Consequently, the customer will opt for new battery packs, and eventually, the operating time of battery packs will be greatly shortened. In addition to that, owing to the mentioned benefits, battery packs will be owned by BSS rather than vehicle owners. This may originate anxiety for users because of not possessing the battery at the time of purchasing the EV and they may be prejudiced against the leasing model.

Application of battery swapping technique for public transportation, most especially for the public transit electric buses, is worth mentioning since it may find a way out the challenges that BSS of private electric vehicles encounters. The characteristic features of electric buses and their corresponding advantages are stated as follows; firstly, they travel over predefined routes with a predefined timetable, which provides BSS the opportunity to establish a more feasible controlled charging strategy and to ease deciding the optimal locations of it while minimizing the number of stations needed. Secondly, public bus fleets are composed of a predefined and a certain number of buses with limited models. These features eliminate the problem related to the lack of standardization of the battery packs, and also accurate sizing of the station is ensured. Thirdly, the increase in the number of buses over time is obviously fewer than the growth of private vehicles. Consequently, the former can be compensated by only expanding the existing stations.

Table 1.1 provides further analysis that shows the strength and weakness of the battery swapping technique comparing to conductive and inductive charging.

STRENGTHS	WEAKNESS
- Scheduled battery charging to achieve a controlled charging strategy. - The sticker price of EVs is reduced as the cost of the battery is not included. - Battery charging process is scheduled to minimize the electricity cost - The profit is increased by participating in electricity markets by injecting power into the grid and also providing secondary services: spinning reserve, voltage support, and demand response. - Possibility of postponing the battery charging to the nighttime or off-peak hours. - The concern related to battery life is relieved since an advanced and healthy control strategy can be run by BSS to avoid sequential damages. - Longer trip distance is ensured by accessing easily the fast battery swapping in the BSS. - Having a large parking space is not necessary and eventually, this reduces the cost of the real estate. - The charging is speeded up which would become as fast as refueling a gasoline-powered vehicle. - BSS behaves as a large flexible load in the power system. - EV owners don't need to upgrade their household infrastructure to high power charges. - The price of the battery and its associated facilities will significantly drop due to the rapid development of battery technology and this will cause the BSS to be more practical. - The potential overloading to the grid or peak demand is avoided by controlling the charging time of the batteries. - Easy adaption for public transportation. - High level of autonomy and communication between the smart vehicle and station can be achieved.	- The lack of standardization of EV battery packs. - The arrival rate of private EV owners is stochastic and unpredictable. - Lack of standardized battery pack design that allows easy and rapid disconnection and reconnection from the vehicle. - The location of battery packs must be easily accessible - High initial investment required to build complex infrastructure and to purchase special swapping equipment. - Customer acceptance of leased/rented battery packs model. - Commercially viable business models are absent. - New battery packs will be favored by customers which would decrease the operating cycle of any battery pack. - Accurate value of the State of health and state of charge of the battery packs may not be estimated properly. - Sizing the station; estimation of the total number of charging bays, batteries, and logistic equipment must be chosen in advance.

Table 1.1 Strengths and weaknesses of battery swapping technique

1.4 Electric Vehicles Charging Rules

The battery pack (also known as a traction battery) is the component of an EV that stores electric energy and delivers the power to the electric motors. These batteries are rechargeable (secondary) batteries, which can be recharged from the electrical power distribution grid. The battery pack is equipped with individual battery cells whose nominal voltage is limited (e.g.3-4 V). For this reason, to achieve the desired voltage capacity (e.g.400-800V) and amp-hours (Ah) of an EV in the final pack, many hundreds of cells are connected in series and parallel configurations. In general, a fixed number of cells are arranged in battery modules that protect them from external factors i.e. vibration, heat, or shocks. As an example, Tesla Model S has a total of 7104 battery cells that are structured in 74 cells in a parallel-group,6 groups in series for a module, and 16 modules in series. (444 cells in a module x 16 modules=7104 cells in total). One can find several different types of batteries that EVs utilize such as Nickel Metal Hydride (Ni-MH), Lithium-Ion (Li-Ion), Molten Salt (Na-NiCl2), Lithium Sulphur (Li-S). Li-Ion batteries are the most used technologies in the current battery market owing to outstanding performance in terms of increased power density(800 … 2000 W/kg) and energy density (100 … 250 Wh/kg) which enable the production of batteries with decreased dimensions and weight, showing the best solution for "charge to weight" parameter. Prolonged life cycle due to lack of memory effect(keeping the energy capacity at maximum and unaffected level after several recharging and discharging operations), moderate energy consumption(14.7kWh/100km), a decreasing trend in the cost value, and progressive manufacturing technology are the other advantages that make Li-Ion batteries appropriate choice in this area [10].

The main parameter that quantifies the charging time level is the charger power level, and consequently, the International Standard in Europe(defined by the International Electro technical Commission (IEC)) and in North America(defined by the Society of Automotive Engineers (SAE)) both referred to this parameter to establish the standards for the classification of EV charging methods. IEC makes the classification using the term 'mode' and

it defines four modes to charge EVs with different rated powers and so of the time of recharge. Similarly, SAE uses the term 'level' and it is composed of three levels [11]. Tables 1& 2 illustrate each mode and level by highlighting the level of voltages, maximum current levels, the type of power (single-phase or three-phase AC, DC), the maximum power ratings, and lastly estimated charging time ranges. Since the development of DC fast charging systems still continues, it is possible to observe increased charging rates for mode 4 and level 3. These are called ultra-rapid DC chargers and typically they provide power at up to 350 kW. (typically, either 100 kW, 150 kW, or 350 kW). It must be pointed out that different strategies can be adapted to charge the battery pack in practice than the ones highlighted in the tables.

Level	Power Supply	Voltage Level[V]	Max Current[A]	Power[kW]	Location	Charge Time
Level 1	1-phase AC	120 V AC single-phase	16	1,9	Domestic	Slow
Level 2	1-phase AC	240 V AC single-phase	32	7,7	Semi-Public	Fast
	1-phase AC	240 V AC single-phase	60	14,4	Semi-Public	Fast
	3-phase AC	400 V AC three-phase	32	22	Semi-Public	Fast
Level 3	DC level 1	450 V	<=80	< 50	Public	Rapid
	DC level 2	450 V	200	90	Public	

Table 1.2: IEC EV charging modes based on IEC 61851-1[11-13]

Mode	Power Supply	Voltage Level[V]	Max Current[A]	Power[kW]	Location	Charge Time
Mode 1	1-phase AC	230 V AC single-phase	10 - 16	≤ 3,7 kW	Domestic	Slow
Mode 2	1-phase AC	230 V AC single-phase	16	3,7 kW	Semi-Public	Slow
	3-phase AC	400 V AC three-phase	32	22 kW		Fast
Mode 3	3-phase AC	400 V AC three-phase	> 32	> 22 kW	Public	Fast
Mode 4	DC level 1	500 V	80	40 kW	Public	Rapid
	DC level 2		200	100 kW		

Table 1.3 Levels of EV charging according to SAE [11-13]

The charging speed is highly dependent on the charger power level however, there are also, several factors that may affect charging speed and eventually charging time.

Size of battery: The vehicle's battery capacity is measured in kWh, and the higher its value makes the charging time longer.

Vehicle	Battery	3.7kW slow	7kW fast	22kW fast	43-50kW rapid
Mitsubishi Outlander	13.8kWh	4 hrs	4 hrs	4 hrs	40 mins
Nissan LEAF (2018)	40kWh	11 hrs	6 hrs	6 hrs	1 hr
Tesla Model S (2019)	75kWh	21 hrs	11 hrs	5 hrs	2 hrs

Table 1.4 Effect of battery capacities on charging times [14]

State of charge(battery): Initial level of battery percentage has an impact on the charge speed. Figure 1.6 shows an example of a charge curve. Charge speed can be found on the y-axis, and it is expressed in kW, and SoC can be found on the x-axis, and it shows how full the battery is. It can be observed a decreasing trend in charge speed starts when the SoC becomes 70%, and the decrease becomes sharper when more charging is applied. It must be underlined that charging above 80 to 90% of the battery packs is not needed since charging time gets progressively longer.

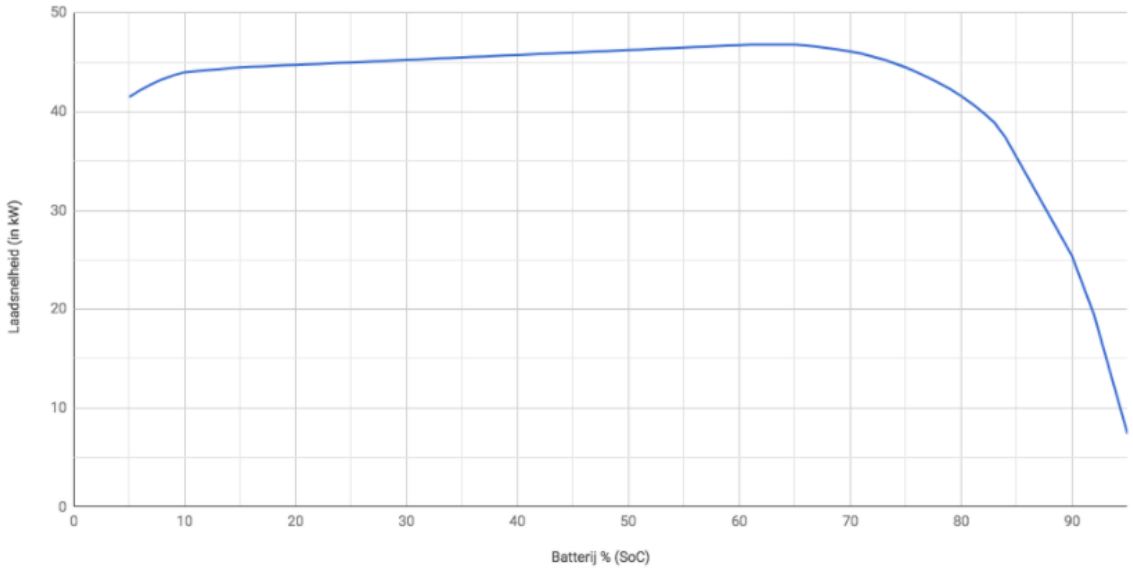

Figure 1.6: Influence of battery percentage on charge speed [15]

The maximum charging rate of vehicle: A vehicle's battery can be charged at the maximum charge rate the vehicle can allow. As an example, having a vehicle's max charge rate of 7kW, there is no way to charge any faster by utilizing a 22-kW charge point.

The maximum charging rate of charge point: The duration of charging will also be dependent on the maximum charging rate of the charge point that is used. For instance, even if your vehicle can charge at 11kW, it will only charge at 7kW on a 7kW charge point.

Environmental factors: The internal resistance of the battery grows with the decrease of temperature and the maximum voltage level is reached earlier if the same current level would be applied. To prevent damage of higher voltage on the battery, the charging current must be reduced and that's why colder ambient temperature keeps the charging duration longer, particularly in the case of using a rapid charger. Additionally, colder temperatures decrease the efficiency in a way that fewer kilometers are added per time charging. At higher temperatures(>+40°C), the internal resistance of the battery drops further which leads to better charging performance but increased chemical activity due to higher temperature may cause self-discharge and battery degradation. Figure 1.8 demonstrates the charging time of Li-ion batteries as a function of different temperatures. It can be seen from the plot that charging time gets the best results at elevated room temperatures(25°C-40°C). At 5°C, charging takes place in 1.5h compared to 1h at 40°C. Charge power must be reduced by half at temperatures higher than 50°C due to safety concerns such as hazardous temperature rises in battery and at freezing temperatures to avoid anode degradation [16].

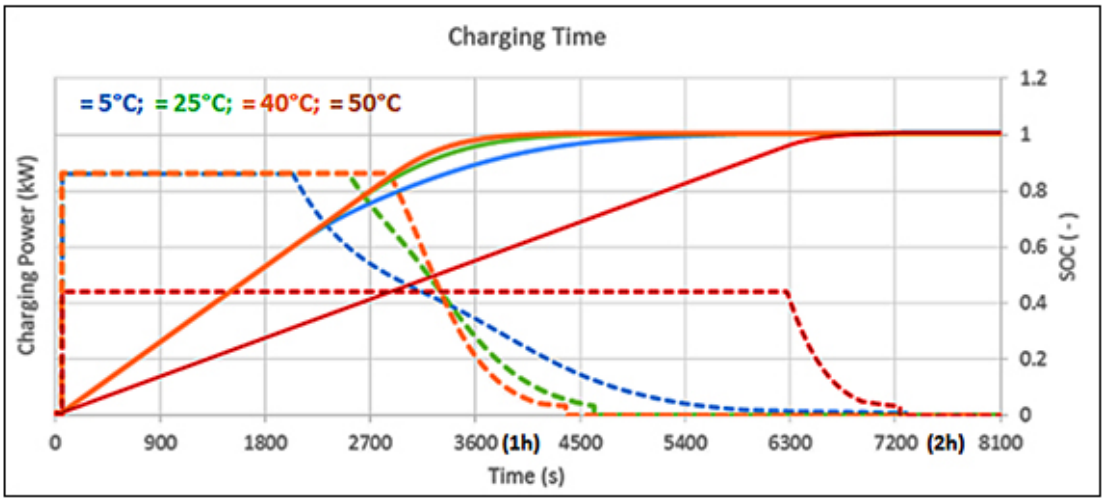

Figure 1.7: Charge time as a function of temperature and SoC [16]

To find a precise charging time, several factors must be taken into consideration such as the state of health of the battery, maximum power output behavior during the charging cycle, and charging strategy (constant voltage mode or constant current mode). However, it is possible to find an estimated charging time by knowing the parameters including the vehicle's battery capacity indicating how much energy can be stored(measured in kWh), state of charge of the battery which represents a relative charge that is present in a battery relative to its total capacity, environmental conditions, and the maximum available charging power which quantifies how much energy is transmitted by charging station to battery pack per unit of time(measured in kW) and it will be limited by the lowest power level found in charging grid points or on-board charger of the electric vehicle. As a result, the estimated time to charge a battery that has a partial capacity, or zero charges can be calculated by subtracting target charge capacity by current charge capacity and then divided by relevant maximum charging power. The formula also includes a coefficient that counts to the occurred power loss during the charging operation. Its value depends on the battery temperature, SoH, initial SoC percentage, and charging power and it usually ranges between 80-90% [17-18]. Lithium-ion batteries can have an efficiency exceeding 99% under ideal conditions.

$$ECT = \frac{BC \times TCL - BC \times CCL}{MCP \times \zeta}$$

Where:

-ECT is the Estimated Charging Time [hours]

-BC is the Battery Capacity [kWh]

-TCL is the Target Charge Level [%]

-CCL is the Current Charge Level [%]

-MCP is the Maximum Charging Power[kW]

-ζ is the Average Power Efficiency [%]

Table 1.4 specifies the major players in public transportation, and it indicates the charging powers recommended by each manufacturer for different battery pack capacities. By applying the formula and considering all the different cases, the estimated charging times (from 0% to %100) are calculated.

Brand and Model	Passenger Capacity	Vehicle Dimensions [mm]	Recommended Charging Options by Manufacturers[kW]	Energy Storage System [kWh]	Estimated Charging Times[hours] (0% to 100%)
VOLVO-7900 ELECTRIC-12m	95-(34 seats)	12000x2550x3300	Opportunity Charge-300 kW CCS DC-150kW CCS-AC 11kW 400 V AC	Li-Ion Battery 198/264/330 kWh	300kW➔0.73,0.98,1.23 150kW ➔1.46,1.96,2.45 11kW➔20,26.4,33.33
VOLVO-7900 ELECTRIC-18m	150	17849x2250x3320	Opportunity Charge-450 kW CCS DC-150kW	Li-Ion Battery 264/396 kWh	450kW➔0.66,1 150kW ➔2,3
IVECO E-WAY-12m	27 seats	12060x2550x3350	CCS DC-100kW Overnight at depot 50 kW	NMC battery 280/315/385 kWh	100kW➔3,3.5,4.3 50kW➔6.2,7,8.5
IVECO E-WAY-12m	27 seats	12060x2550x3350	Opportunity Charge-up to 450 kW	LTO battery 73/88 kWh	450kW➔0.2,0.23
IVECO E-WAY-18m	42 seats	17970x2550x3350	Opportunity Charge-up to 450 kW CCS DC-100kW	LTO battery 102/117/250 kWh	450kW➔0.26,0.3,0.63 100kW➔1.13,1.3,2.78
MERCEDES-eCitaro-3 doors- 12m	76-(26 seats)	12135x2550x3400	Opportunity Charge-up to 450 kW CCS DC	NMC- Li-Ion Battery 198/264/330 /396 kWh	450kW➔0.5,0.66,0.81,1 150kW ➔1.5,2,2,5,3
MERCEDES-eCitaroG-4 doors-18m	136-(41 seats)	18125x2550x3400	Opportunity Charge-up to 450 kW CCS DC	NMC- Li-Ion Battery 264/330/396 kWh	450kW➔0.66,0.81,1 150kW ➔2,2,5,3

Table 1.5 Charging parameters of major electric bus manufacturers

2 State of Art

This chapter provides recent techniques to operate the battery exchanging/charging station that is adaptable for public transit. The detailed drawings of the station with its members and the operating cycle of the station are illustrated. Also, the relevant scientific studies that have been done to enhance the battery swapping technique for public transportation are reported.

2.1 Battery Exchanging Mechanism for Public Transportation

The three consecutive patents filed by Kookmin University Industry Academy Cooperation Foundation [19-21] derive the inventive concept of battery swapping for EVs and the application of the invention on the electric bus. The technical drawings of the station and their brief descriptions are stated as follows.

Figure 1.8 gives a schematic configuration that explains how the battery is removed from the electric bus and how it is placed on charging racks in accordance with replacing robots. Figure 1.9 shows the automated robot that has three tasks: dismounting the depleted battery from the vehicle, placing it to the charging racks, transporting the charged battery, and mounting it to the vehicle. Figure 1.10 reveals the interior view of the station where charging racks are located. Figure 1.11 represents the exterior structure of the station where several simultaneous swapping operations are accomplishable.

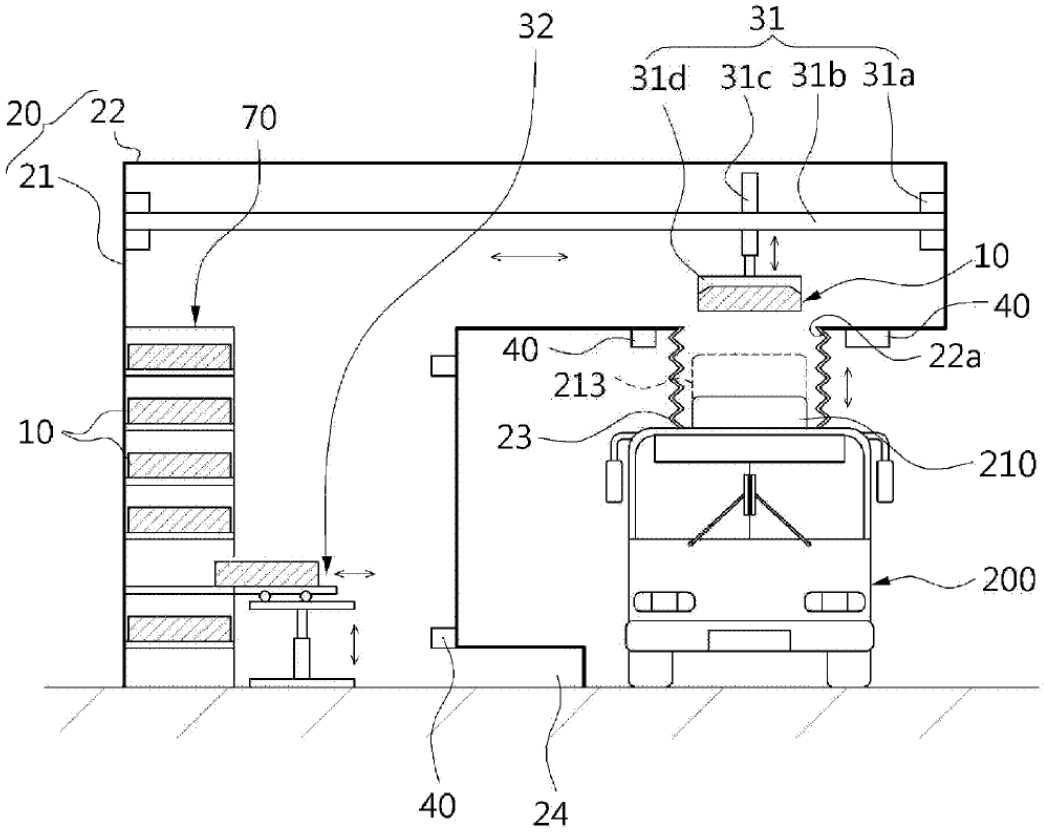

Figure 2.1: Schematic configuration of battery exchanging type charging station [19]

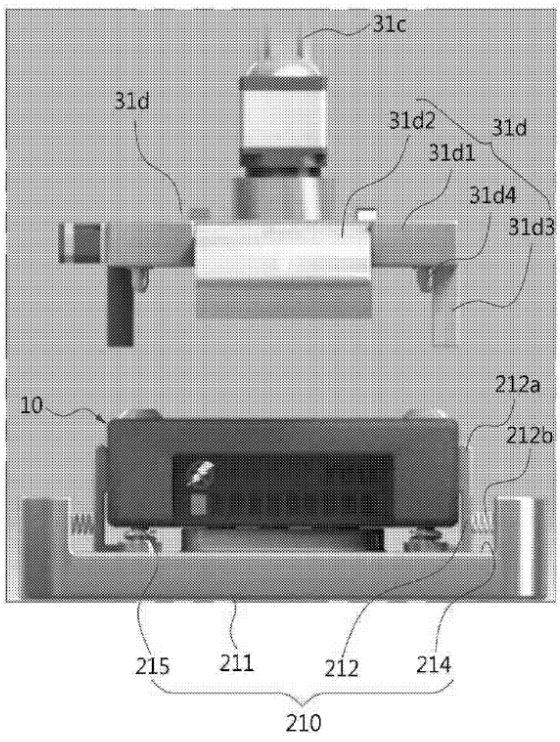

Figure 2.2: Structures of battery replacing robot and battery mounting module [19-20]

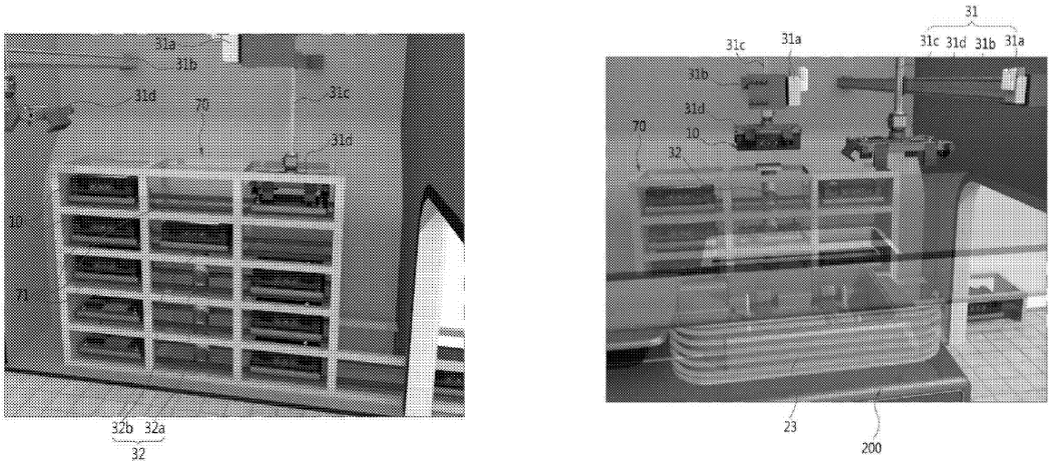

Figure 2.3: Interior structure of the station [20]

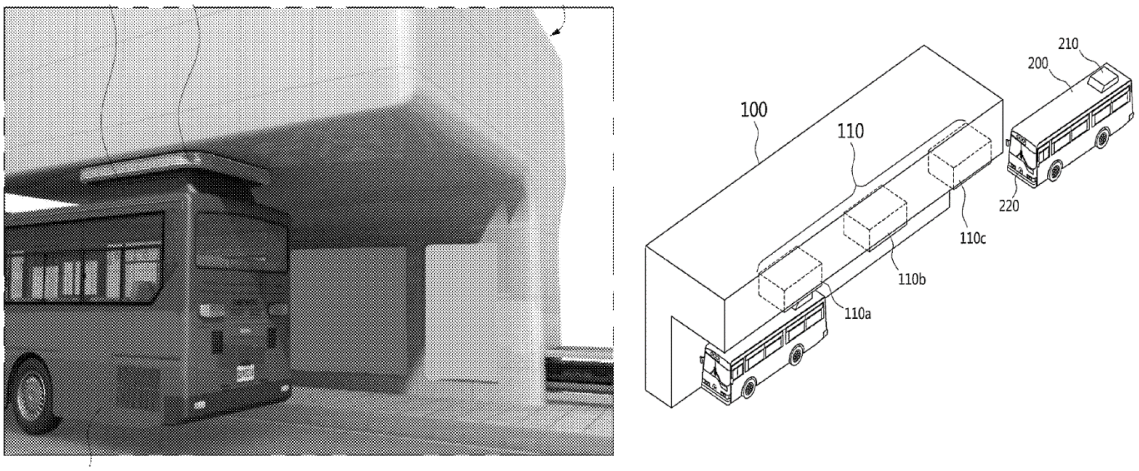

Figure 2.4: Exterior structure of the station [20-21]

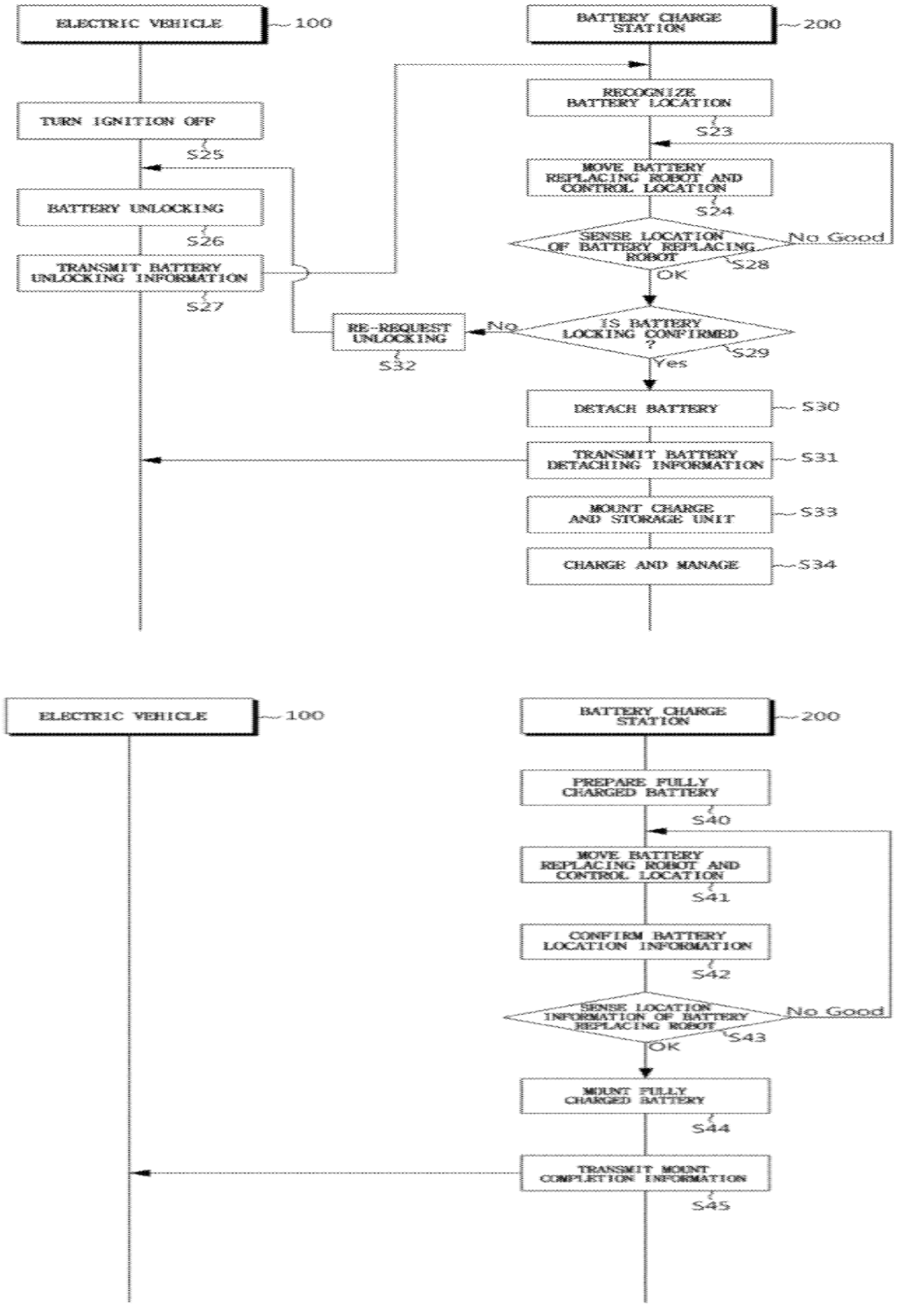

Figure 2.5: Information flow between EV and station [19]

The sequences of the battery exchanging method are described as follows.

1-Protection cover of a battery mounting module that is located on the upper part of the EV is opened.

2-The signal that informs the opening of the protection cover is sent to the battery swapping station.

3-The locking unit of the depleted battery is released by the electric vehicle.

4- The signal that informs unlocking is transmitted to the battery swapping station

5-BSS uses the image sensor to determine a mounting location.

6-The depleted battery is ejected from the seating base of the mounting module and is moved to charging racks by a battery replacing robot.

7- A Prepared fully charged battery is mounted on the seating base of the mounting module.

8-Battery mounting completion signal is sent to EV from station.

9-The fully charged battery is locked by EV after confirmation of the connection of the battery.

2.2 Relevant Researches on Public Transportation

The research [22] published by the Department of Automotive Engineering, Kookmin University introduces the application of electric buses equipped with roof-top mounted battery exchange systems as a suitable solution for public transportation. The study suggests the development of an energy model to simulate the energy consumption of the electric buses operated within the battery exchange system. The model is built in accordance with the driving cycle and the specifications of the electric powertrain, battery pack, and HVAC system. The model is validated by comparing the estimated energy consumption obtained in the simulation with experimental data obtained from the pilot program built in the city of Pohang, Korea with two battery exchange stations and three electric buses. The validated energy

model can be used as a preliminary analysis tool to check the feasibility and to measure the performance of the planned battery swapping stations for public services.

In the published article [23], the electric public transport system is planned and designed under battery swap mode and it suggests improved strategies for scheduling and routing of electric bus fleets. According to swapping and charging demand analysis, an algorithm is developed to optimize the sizing of BSS, the number of battery packs, charging system, and power output. The method is validated by a numerical simulation that evaluates the operations of the case study of Xuejiadao Station-China serving six routes. The objective of the study is to accelerate the wide adoption of BSS.

The localization problem of battery swapping stations for electric buses on traffic networks and the minimization problem of the number of stations are analyzed in this research [24]. To address the mentioned issues, three programming models are developed namely, path-based model, set-covering-based model, and flow-based model. The application of the models and their testing is executed in the city of Seoul.

The case study of TRANSDEV [25] presents challenges of the employment of the electric buses and proposes plans to overcome them. Having regard to the increase in the number of EBs and the size of their batteries, the impact on the grid is expected as a result of the charging the EBs fleet. The paper develops an optimization algorithm that enables a smart charging methodology to cope with the problems related to the charging infrastructure while considering the issues of battery aging, charging cost, and load power variations.

In [26], the adoption of electric-powered buses into the public transportation system is presented in terms of economic aspects. The cost-benefit analysis is derived from the developed economical model.

3 Model Development

The thesis aims to alter the current public transportation system in the city of Turin with an electrified transportation system that can be managed under the battery swapping method. To practice this scenario, discrete event modeling and simulation are used to design BSS and evaluate its key performance parameters. The simulation model is built in compliance with the in-depth research conducted on Turin's public transport. In this chapter, the steps of the model building process and all the assumptions involved in the model building will be illustrated and ultimately, the development of the simulation model will be discussed.

3.1 Model Building

The number of circulating buses at different hours and their routing characteristics are essential to estimate the daily battery swapping service demand and optimize the sizing of BSS. The characteristics of public transportation in the city of Turin are obtained from the website of GTT (Gruppo Torinese Transporti), the local transport company, that is responsible to provide the public transport service in Turin [27]. GTT offers real-time traffic monitoring for each bus line. By accessing each line between the hours of 8.00 am and 12.00 am, the total number of circulating buses at different hours of the day are found. The obtained data are demonstrated in Figure 3.1. It can be seen that the total number of buses reaches its maximum value between 8.00 am-10.00 am and its minimum value in between 10.00 pm-12.00 am. No significant difference can be observed from 10.00 am to 10.00 pm and it shows a steady behavior with a mean value of 419 buses. The average number of buses circulating per each line and their routing characteristics will be used to establish the arrival schedule for BSSs when the simulation model is developed.

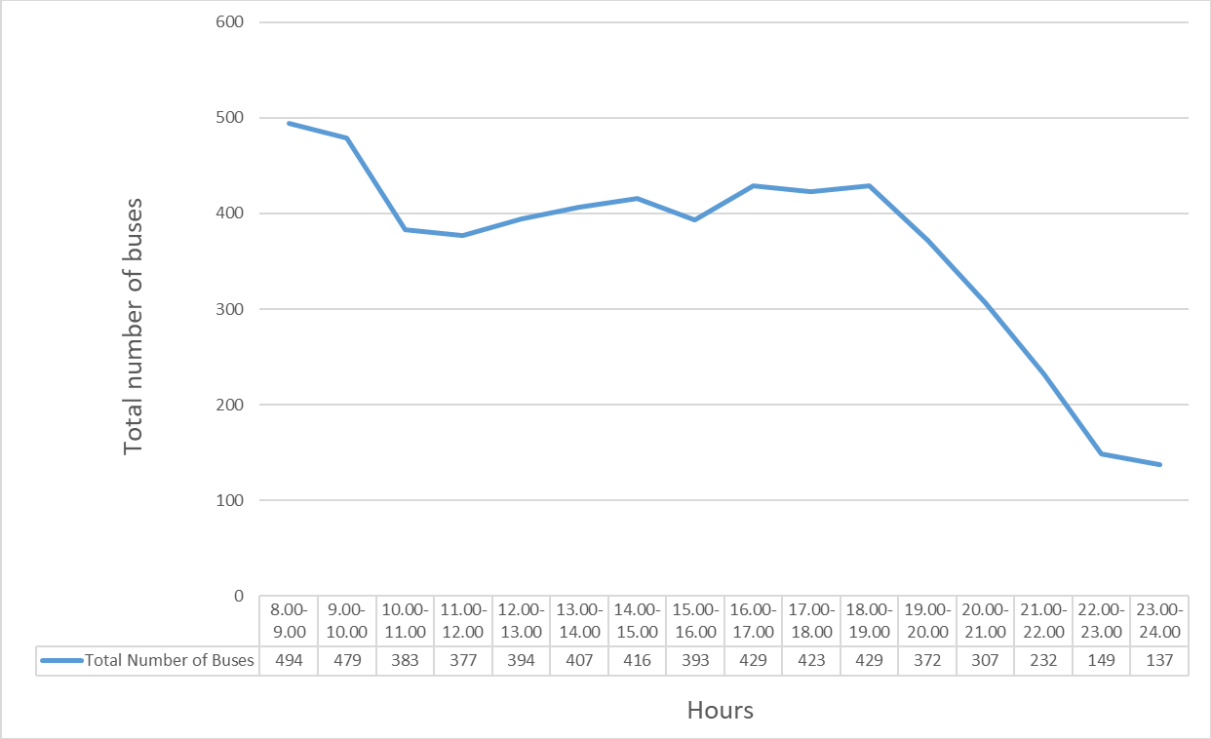

Figure 3.1: The circulating buses on the road in different time slots in Turin

GTT manages the following three distinct public transport networks: Urban network, if the journey begins and ends within the urban zones only, Suburban network if the journey begins and ends within the suburban zones only, Interurban network if the route begins in the urban section and ends in the suburban section or vice versa. Table 3.1 demonstrates the distribution of the lines among each network, and it shows the average number of buses circulating per day for each network. As can be seen from the table, Urban and Suburban networks show the same characteristics in terms of average round trip distance traveled and it is slightly less than the average round trip distance of the Interurban network. Therefore, it has been decided to work with two different electric buses that are produced by the major bus manufacturers and eventually two different battery packs whose characteristics are stated in Chapter1.4-Table 1.5. The first battery pack belongs to Volvo 7900E-12 m that has a capacity of 198 kWh and it will be used for Urban and Suburban networks. Since the Interurban network requires a slightly longer range, a battery pack that has more capacity than the first battery pack is chosen. The second battery pack belongs to Mercedes e-Citaro 12m that has a capacity of 264 kWh and it will be used for Interurban networks. In conclusion, arriving battery

packs will be divided into 53% (47,49%+5,49%) Volvo 7900E for Urban and Suburban networks and 47% Mercedes e-Citaro for Interurban networks.

Network	Number of lines	Percentage	Average # of buses per day	Percentage	Average km traveled
Urban	42	40,78%	199	47,49%	18,91093023
Suburban	14	13,59%	23	5,49%	18,66357143
Interurban	47	45,63%	197	47,02%	25,05137255
Total	103		419		

Table 3.1 Characteristics of transportation networks

Figure 3.2: Volvo 7900E-12m-198 kWh battery pack

Figure 3.3: Mercedes-eCitaro-12m-264 kWh battery pack

What is the average energy consumption of these chosen electric buses? This is one of the most important parameters that must be addressed since it highly affects the range of an electric bus on one charge. In the simulation model, the SoC of each bus will be updated when they complete one trip according to the average energy that they consume per kilometer and when they reach the threshold SoC percentage, they will be directed to BSS for swapping operation. Therefore, its value has to be decided precisely since the arrival scheduling of

electric buses to the swapping station can be estimated by using this parameter. Surely, there are some external factors that may influence the energy consumption of electric buses namely, outside temperature, the use of air conditioning systems, and most importantly heating. Last but not least, driving behavior and road conditions are significant as well. To come up with average energy consumption data of the electric buses, a deep research has been executed, and a dedicated report on e-bus performances was released by Viriciti which is a Dutch telematics company. After a ten months-long connection of data across all seasons, more than one hundred e-buses (79 12-meter buses and 27 18-meter buses) from different OEMs were analyzed across seven cities in the Netherlands. The results indicate that 1.15 kWh/km is the average energy consumption for the 12-meter vehicles, whereas 18-meter buses consume average energy of 1.63 kWh/km. Additionally, the report reveals the effect of cold and hot weather conditions on the e-bus energy consumption. As can be seen from Table 3.2, it can be noticed that consumption increases for both 12-meter buses and 18-meter buses during the winter and summer seasons of the year. The reason that we observe higher energy consumption during colder months of the year compared to summer months is the extensive power use caused by the electric heater for a warm-up period of the buses and it is more than the power drain of an air conditioner in hot months. Also, a higher amount of drag is generated between tires and road especially in non-urban areas where higher speed can be reached, and no obstacles can be observed [28].

Time period: **01/06/2019-31/03/2020**	**Number of buses**	Difference in consumption between **Normal and Cold** temperatures	Difference in consumption between **Normal and High** temperatures
12m buses	**79**	**14%** ▲ in cold temps	**9%** ▲ in high temps
18m buses	**27**	**21%** ▲ in cold temps	**12%** ▲ in high temps

Table 3.2 Effect of weather conditions on energy consumption [28]

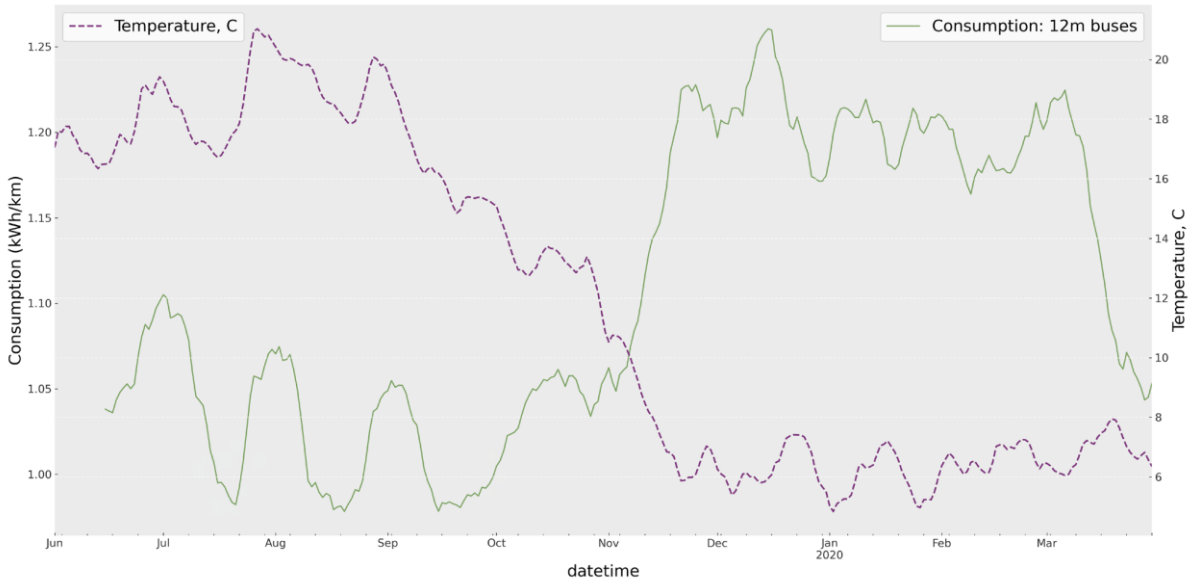

Figure 3.4: Correlation of temperature and daily average energy consumption of 12m buses [28]

The simulation model will consider only the fleet of electric buses belonging to the same corporation and it will not simulate the behavior of the private electric vehicles. Therefore, it is possible to establish a set of criteria for the expected value of SoC (level of charge of an electric battery relative to its capacity) at which electric buses arrive at the battery swapping station. The threshold value of the expected SoC percentage is set as 25% which means when the remaining battery capacity of each bus relative to its maximum capacity reaches 25%, they will be redirected immediately to BSS for swapping service.

The depleted batteries will be placed in the charging racks where charging of each battery pack will take place with the help of localized AC-DC converters that deliver DC power to all the chargers. Recommended charging options for battery packs are provided by each electric bus manufacturers in Chapter 1, Section 1.4. A common charging technique recommended by both manufacturers is chosen for both battery packs, and it is CCS (Combined Charging System)-DC fast charging that provides a maximum charging power of 150 kW. As it is explained in the section of electric vehicles charging rules, charging the battery packs above the SoC percentage of 80% results in progressively longer charging times. For this reason, each battery pack will be charged to a maximum state of charge percentage of 80% starting from a minimum SoC level of 25%. To calculate the estimated charging time for both battery packs,

all the factors that have been mentioned in Section 1.4 will be taken into considerations. In compliance with estimated charging time formula, the first battery pack with capacity of 198 kWh will require 50 minutes to raise its SoC level from 25% to 80%, in the meantime, second battery pack with capacity of 264 kWh will require 65 minutes to reach to the decided maximum SoC level.

3.2 Defining Model Assumptions and Parameters

In this section, the assumptions that are considered during the simulation model development and the parameters used in the simulation model are reported.

Assumptions:

- Swapping stations will operate only on weekdays from 8.00 am to 12.00 am considering that no public transport service will be provided after 12.00 am and circulating buses are dropped significantly at the weekends.
- Battery degradation (Loss of efficiency) due to fast charging and the high number of charging-discharging cycles is not taken into consideration. The model assumes the replacement of malfunctioned batteries with fresh ones by the station management.
- The model considers only public electric buses and not the private electric vehicles.
- The type of chosen batteries are both Lithium-Ion batteries.
- Charging time of Li-ion batteries gets the best results at elevated room temperature and that's why the station and charging racks are kept at the temperature of 25°C-40°C.
- The operating principle is defined as FIFO (First in First Out) in which the vehicle arriving first gets the swapping service earlier compared to those who arrive later.
- The number of operating buses for each line varies hourly according to their scheduling. The model considers the average number of operating buses circulate for each time slot.

- The model does not consider the regenerative braking which is an energy recovery mechanism or neither any traffic conditions.
- Maintenance operations or breakdown events are not included in the simulation model.
- The simulation will be initiated with batteries in the warehouse having the SoC level equal to 80%.

Parameters:

- The number of charging racks will be the same as the number of batteries that the warehouse can hold.
- Charging power is equal to 150 kWh.
- Average charging efficiency that counts the occurred power loss during the charging operation is equal to 0.9.
- Expected SoC percentage is set as 25 %.
- There will be two types of arriving battery packs: Type 1(198 kWh) and Type 2(264 kWh) with the proportions of 53% and 47% respectively.
- To charge the Type 1 and Type 2 battery packs from 25% SoC to 80% SoC with charging power of 150 kWh require charging times of 50 minutes and of 65 minutes respectively.
- The battery packs in the charging racks maintain the same proportions as the case of arriving battery packs.
- Each battery pack will be charged to a maximum SoC percentage of 80%.
- 1.15 kWh/km is the average energy consumption for the 12-meter vehicles in normal temperatures. Its value raises to 1.311 kWh/km during the cold months of the year and to 1.2535 in hot temperatures.

	AGV	ASRS
Task Executers Speed(x axis)	1 m/s	2 m/s
Task Executers Acceleration and Deceleration	0.5 m/s^2	0.5 m/s^2
Load Times	9 s	9 s
Unload Times	9 s	9 s
Capacity	1	1
Lift Speed(z-axis)	-	0.23 m/s
Extension Speed(y-axis)	-	1.2 m/s
Initial Lift Height	-	3 m

Table 3.3 Parameters of transport vehicles used in simulation model

3.3 Development of Simulation Model

The simulation model is created with reference to the model designed by Eng. Stefano Locardo [29]. His model was designed to simulate the battery swapping station for electric vehicles and the modifications have been performed to adopt the mentioned model for public transportation. In this section, the steps to construct the simulation model and utilized codes will be explained.

Arrival Prediction Model developed by Anylogic:

In this first step, before proceeding with the Flexsim model, an initial simulation model is created by a different simulation modeling tool called Anylogic and it is executed to predict the hourly battery swapping demand for public transportation in the city of Turin. Anylogic is an agent-based modelling software. Agents can be considered as the units of the model design and they are the main blocks that are used for building the Anylogic models since they can be representative of various elements in the model including people, vehicles, equipment, non-material things, or organizations. It is possible to assign behavior, history, timing, or contacts to any agent in the model, and also, the software enables the user to define variables, events, state charts, or flow charts within an agent. The unique feature of the Anylogic is the possibility of importing GIS (Geographic Information System) capabilities into the software to give the

users rich and interactive functionalities such as the movement of agents with a particular speed from one place to another using the specified routes and passing them through the processes defined by flowcharts, action execution upon arrival, and other useful services. The creation of the agents was the first step to construct the model and there are mainly three agents namely; the deposit center where the buses start their travel, the battery swapping station where they receive swapping service, and lastly the electric buses which have been created as a population of agents of the same type for different lines. Then, to build a regional transportation network for each line, the agents have been converted to the GIS points and have been positioned on the Turin's map as illustrated in Figure 3.5. The location of the deposit center has been founded from the website of the GTT and the initial locations of the buses coincide with the location of the deposit center. The BSSs have been located in the boundary between the urban and suburban regions so that both the urban buses and suburban buses can reach the stations without facing any problems in terms of running out of battery. Additionally, since it was not possible to simulate the movement of electric buses in any traffic conditions and the software has no feature to simulate the deceleration or acceleration, the speed of the electric buses was determined as a constant value of 10m/s.

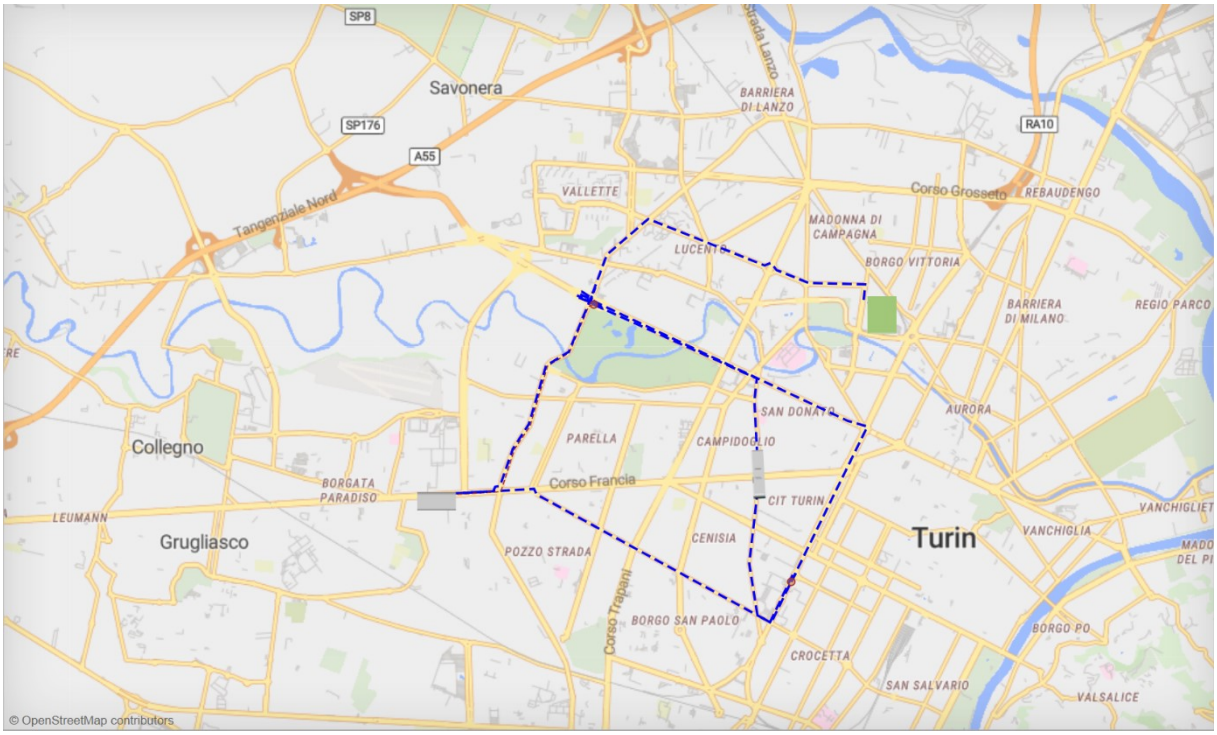

Figure 3.5: Regional transportation network defined by Anylogic

The first and lost stops of the lines have been added to the map not as agents but as GIS points. By doing so, various lines have been simulated by only varying the first and lost stops of each line. The agents and the GIS points on the map are connected by the GIS routes that employ the real roads with exact distances. Moving the agents which are electric buses in our case was the next step in the simulation. To do this, a code was necessary to create a Route Provider to set it as a route source for the agents. A custom code called 'getCustomRouteProvider' which is a function that makes the buses follow along the given GIS routes on the map has been created and it specifies any route drawn on the GIS map as an argument of the function of "getCustomRouteProvider(). In Anylogic, normally the agents choose to move along the shortest or fastest route of the network to reach the destination when the starting locations (Deposit center or first stops) or the target locations(BSSs or last stops) are selected as GIS points on the map. To avoid this issue and to make agents follow the specific routes, the agent that must be moved needs to place in the coordinates of starting point of the motion which are defined by the latitude and longitude of the 'GISSTARTPOINT' and it must be moved to final coordinates using the get function which locates the final

destination coordinates '(GISFINALPOINT.getLatitude(), GISFINALPOINT.getLongitude())'. The mentioned code was reported below, and it is written in Java coding language since Anylogic is fully mapped into the Java.

```
return
// Agent moves along the given GIS route
new IGISRouteProvider() {
	@Override
	public Curve<GISMarkupSegment> getPathData(
			double startLat, double startLon, double endLat,
			double endLon) {
		Curve<GISMarkupSegment> curve = new Curve<>();

		for (int i = 0; i < gisRouteAlternate
				.getSegmentCount(); i++) {
			curve.addSegment(
					gisRouteAlternate.getSegment(i));
		}

		curve.initialize();
		return curve;
	}

	@Override
	public double getDistance(double startLat,
			double startLon, double endLat, double endLon) {
		return Utilities.getDistanceGIS(startLat, startLon,
				endLat, endLon);
	}
};
```

In the second place, a state chart as seen in Figure 3.6 has been constructed to define the sophisticated behaviors of the electric buses along their routes and to make them go through the processes defined inside the state chart. It is important to underline that the state chart has been created under the 'Bus Agents' since this is the way to call the functions of state-chart for the agent of buses. Additionally, the parameters and variables are defined under the same section. LineaStartLatitude and LineaStartLongitude are the parameters that locate the first stop of the lines whereas LineaEndLatitude and LineaEndLongitude are used to locate the final destination of the lines. There are 3 variables that are used mainly for the calculation of the SoC. 'DecreaseinSoCinonetrip' is the value in percentage that must be reduced after each bus completes one trip and its value is different for each line since it depends on the traveled

distance of each line and the chosen battery pack capacity. ‘SoCmin’ is the constant variable that works as a threshold value and it is equal to 25%. ‘SoCupdate’ is the variable that demonstrates the SoC value of each battery pack at any time instant and its initial value is 80%.

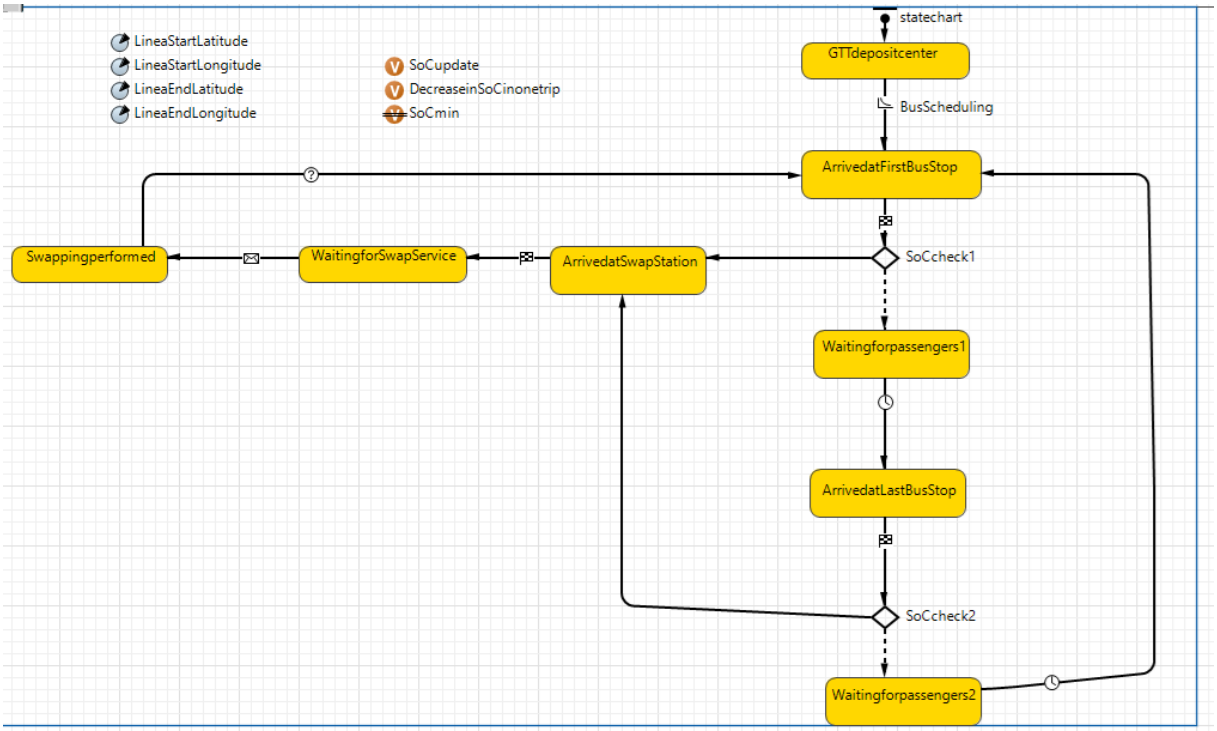

Figure 3.6: Statechart created by Anylogic to predict the arrival rates

Firstly, the entry point of the state chart is used to dispatch the electric buses to their specific lines(routes) with a uniform rate. The transition between the states is triggered by the rate and the functions of ‘setRouteProvider’ and ‘moveTo’ send buses to their starting points of the line. The transition between the state ‘ArrivedatFirstBusStop’ to ‘SoCcheck1’ and ‘ArrivedatLastBusStop’ to ‘SoCcheck2’ are triggered by agent arrival. When each bus completes one trip, their SoC percentage is reduced in proportion to their battery capacities and their trip characteristics i.e. distance covered(km), and afterward, they go through the control processes in which their reduced SoC level is checked whether they maintain sufficient energy level(above 25%). The states of SoCcheck1 and SoCcheck2 have a role to control SoC

level whether they maintain sufficient energy level (above 25%) to retain the public transportation services. It is a 'OR' gate (Conditional State) and when SoCupdate is smaller than or equal to SoCmin, it passes the buses to the 'ArrivedatSwapStation' state. When SoCupdate is higher than SoCmin, it passes them to the 'Waitingforpassengers' states. To represent the buses waiting for passengers at the first and the last stops, two additional states called 'Waitingforpassengers1' and 'Waitingforpassengers2' have been added. Before they start moving from the first and the last stop, states force them to wait for ten minutes before they start moving along their routes and the transitions from these states are triggered by timeout. The functions of 'setRouteProvider' and moveTo are again used to realize the motion of agents between the first and the last stops and they continue their trips consistently between the first stop and the last stop owing to the loop generated in the state chart. When the agents arrive at the state of 'WatingforSwapService', the agents are moved to another process defined under the Agent of SwapStation by using the function of main.swapStation.enter.take(this).

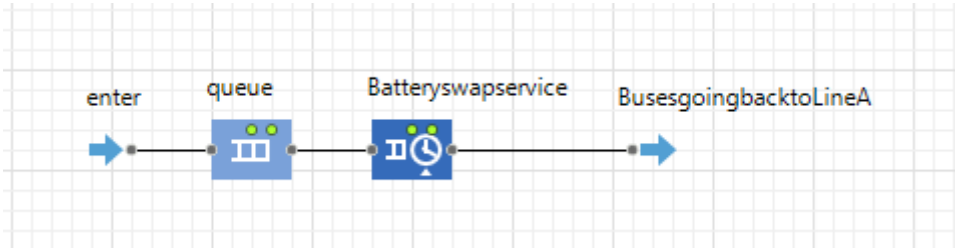

Figure 3.7: Station process chart in Anylogic

This process is intended to replicate the operations of the BSS and to understand the arrival times of the buses to the swapping station by observing the time that agents arrive at the 'Enter' process block. The process includes the queue that keeps the agents individually and the battery swapping service which makes the agents keep waiting 3 minutes, that is the common operation time found in the literature. The exit of the process, 'BusesgoingbacktoLine' is used to send the agents back to the state chart. It sends the following messages: receive("swappedperformed"); send ("swappedperformed", agent) to the state 'WatingforSwapService' and the messages trigger the transition to the state of

'SwappingPerformed'. In this state, after the battery swapping is performed, the value of 'SoCupdate' is raised back to 80% and they are sent back to the first stop in the state chart to sustain their services. In this way, how frequently electric buses arrive for battery swapping at each hour in a day is determined and it is reported in Table 3.4.

	Number of BSS=2		**Number of BSS=3**		**Number of BSS=4**	
	Summer	Winter	Summer	Winter	Summer	Winter
	Number of arriving buses		Number of arriving buses		Number of arriving buses	
Time Table						
08:00-09:00	0	0	0	0	0	0
09:00-10:00	0	0	0	0	0	0
10:00-11:00	4	5	2	3	2	2
11:00-12:00	24	28	16	19	12	14
12:00-13:00	55	65	37	43	28	33
13:00-14:00	75	69	50	46	37	34
14:00-15:00	54	49	36	33	27	25
15:00-16:00	25	29	16	19	12	14
16:00-17:00	36	41	24	27	18	21
17:00-18:00	40	42	27	28	20	21
18:00-19:00	43	39	29	26	22	19
19:00-20:00	56	61	37	40	28	30
20:00-21:00	36	45	24	30	18	23
21:00-22:00	48	39	32	26	24	20
22:00-23:00	41	41	27	27	20	20
23:00-24:00	43	47	28	31	21	23

Table 3.4 Arrival Rates of Buses to Swapping station according to number of BSS and weather conditions

As can be seen from Table 3.4, it is obvious that increasing the number of swapping stations in the city of Turin has a direct effect on the arrival rates at each station. The decreased arrival rates can be observed for 4BSSs and 3BSSs compared to the 2BSSs case. It is interesting to observe that the number of arrivals increases in the winter season as a result of the increased energy consumption. It has been decided to consider only the arrival rates of the winter season in the simulations since it will stress the stations more.

Step 1-Bus Arrivals: As the first step in simulation model development with Flexsim, a fixed resource block that creates flow items has been inserted into the software environment. In our case, it will generate the electric buses arriving at BSSs for swapping service. Flexsim offers three possible operation modes for source blocks: Inter-Arrival Mode, Arrival Schedule Mode, and Arrival Sequence Mode. According to the chosen mode, it creates flow items per an inter-arrival rate, per a scheduled arrival list, or simply from a defined arrival sequence respectively. The Inter-Arrival Mode is preferred since it enables implementation of the same hourly arriving schedules that have been reported previously as in Table 3.4.

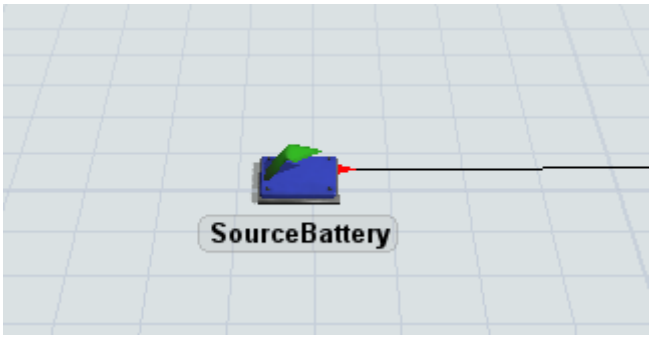

Figure 3.8: Simulation Model Development with Flexsim-Step 1

Step 2-Buses waiting for swapping service

As the large number of buses arriving at the station at the same time slots, an anticipated queue formation is certain. To replicate the buses waiting their turn for swapping service, a queue block has been inserted into the environment and it will store the buses until a downstream object (Swapping platform) accepts them. By default, the queue operates in a FIFO manner, meaning that when the swapping platform becomes available, the bus that has been waiting longest will leave the queue first. Also, the maximum content of the waiting queue is set large enough so that it will not restrict any incoming buses.

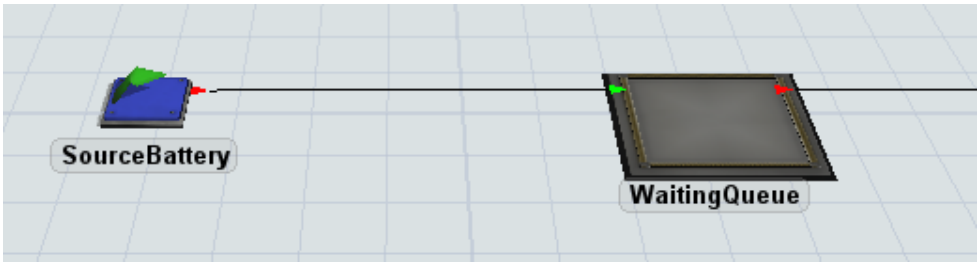

Figure 3.9: Simulation Model Development with Flexsim-Step 2

Step 3-Buses at swapping platform

Another queue has been added to the environment to represent the swapping platform where the depleted batteries are exchanged with the fully charged ones. The maximum number of flow items the queue can hold at a time is set to one because swapping platform can give service to only one bus at once.

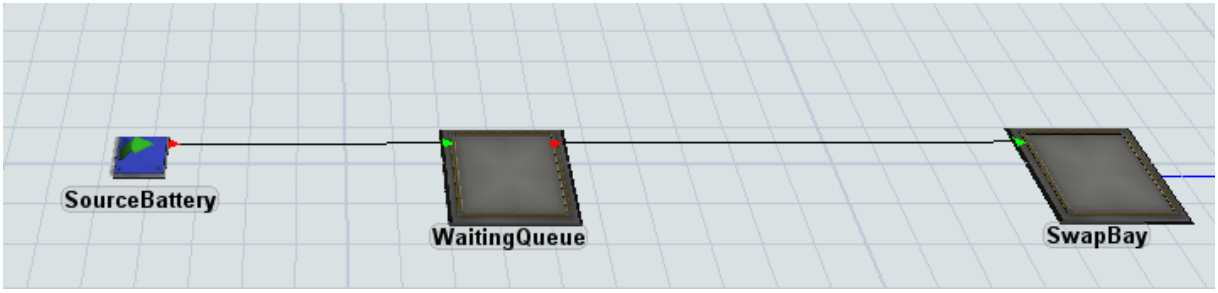

Figure 3.10: Simulation Model Development with Flexsim-Step 3

Step 4-Battery storing and battery retrieval queues

The storing queue is the workstation where automated guided vehicles (AGV) will deposit the depleted batteries temporarily and subsequently they will be moved to charging racks with the help of automated storage and retrieval system (AGRS). Whereas, the charged batteries will be placed on the retrieval queue by AGRS so that they can be transported to the swapping platform employing AGV and they will be inserted into the buses waiting for service.

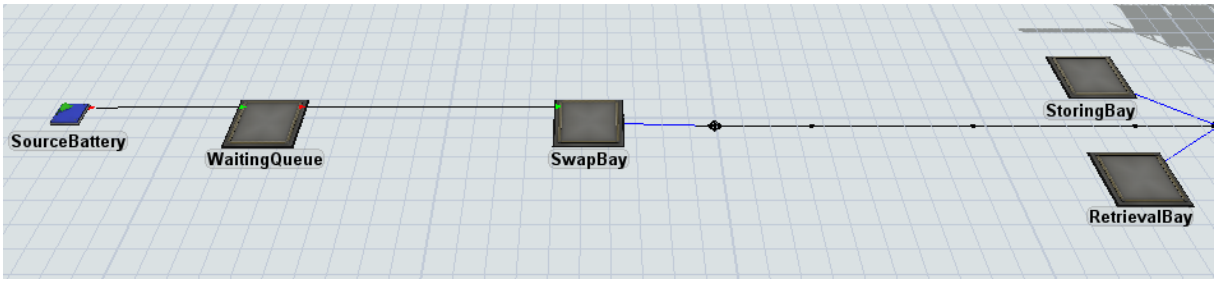

Figure 3.11: Simulation Model Development with Flexsim-Step 4

Step 5-Battery packs in warehouse

At the startup of the simulation, the racks of the warehouse will be filled up with the battery packs that have a SoC level of 80% with the help of a source block, and the proportions of the battery pack types in the warehouse are arranged to maintain the same proportions of the incoming battery pack types. The warehouse is responsible not only to store the battery packs but also to charge the incoming battery packs that are characterized by a low SoC level (25%). Therefore, during the runtime of the simulations, the battery packs that are placed in the racks will be charged to a maximum SoC percentage of 80 % using the maximum charging power available(150kWh) in conformity with the estimated charging time formula reported in Chapter 1.4

.

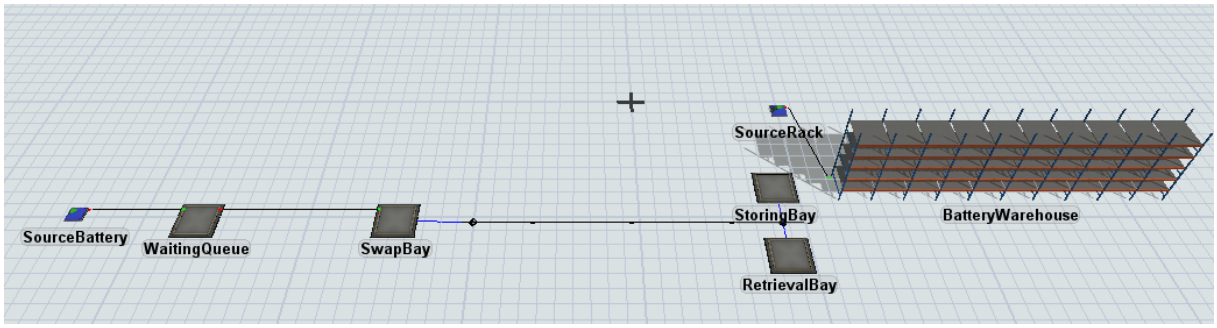

Figure 3.12: Simulation Model Development with Flexsim-Step 5

Step 6-Internal logistic vehicles

The logistics inside the battery swapping station will be taken care of by AGV and ASRS vehicles. AGV will be used to move the arriving battery packs from the swapping platform to storing queue and subsequently to transport the charged batteries from the retrieval queue to the swapping platform. ASRS vehicle will be employed to transport the charged battery packs from charging racks to the retrieval queue and to transfer the arriving depleted battery packs from storing queue to charging racks again. Parameters of mentioned transport vehicles used in the simulation model are reported in Table 3.3 section 3.2.

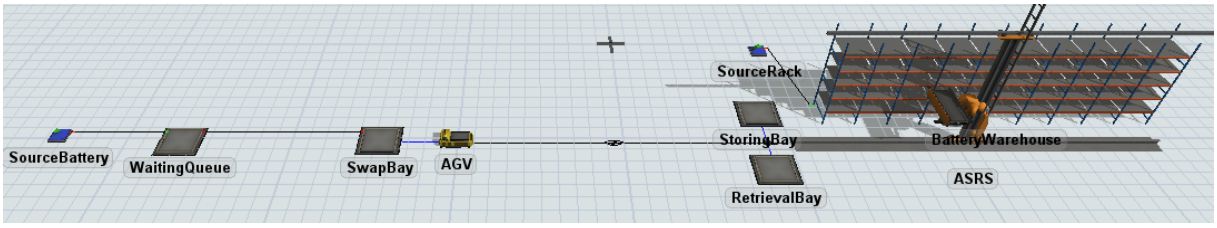

Figure 3.13: Simulation Model Development with Flexsim-Step 6

Step 7-Buses leaving the station

In Flexsim, sink block has the role to dispose of the flow items that are completed their cycle with the simulation model. Therefore, it has been added to the simulation environment to represent the buses leaving the station once they received the swapping service.

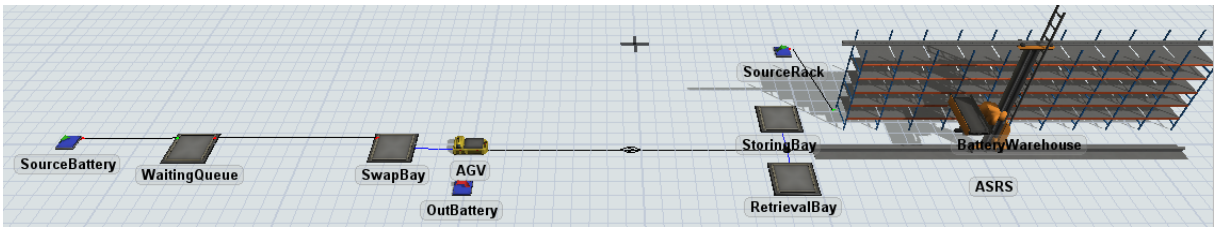

Figure 3.14: Simulation Model Development with Flexsim-Step 7

Step 8-Implementation of coding in simulation model

The code reported below [29] is executed on the creation trigger of the source. It is used to define the characteristics of arriving battery packs such as battery type (Type1 or Type 2),

battery capacity (198kWh or 264 kWh), the battery SoC and more. To assign the values of SoC, the Lognormal Distribution that has a mean value of 25% with a standard deviation equal to 1% is chosen to keep the SoC values of the arriving battery packs as close as possible to 25%. To maintain the decided proportion of the type of the arriving battery packs, Bernoulli Distribution (53, 1, 2) that assigns 53% of the batteries as Type 1 and 47% of the batteries as Type 2 is employed.

```
Object current = ownerobject(c);
Object item = param(1);
int rownumber = param(2); //row number of the schedule/sequence table

{ // ************* PickOption Start ************* //
/***popup:SetLabel*/
/**Set Label*/
Object involved = /** \nObject: *//***tag:object*//**/item/**/;
string labelname = /** \nLabel: *//***tag:label*//**/"Type"/**/;
Variant value = /** \nValue: *//***tag:value*//**/bernoulli(53, 1, 2,
getstream(current))/**/;

involved.labels.assert(labelname).value = value;
} // ******* PickOption End ******* //

{ // ************* PickOption Start ************* //
/***popup:SetLabel*/
/**Set Label*/
Object involved = /** \nObject: *//***tag:object*//**/item/**/;
string labelname = /** \nLabel: *//***tag:label*//**/"SoC"/**/;
Variant value = /** \nValue: *//***tag:value*//**/lognormalmeanstdev(25, 1,
getstream(current))/**/;

involved.labels.assert(labelname).value = value;
} // ******* PickOption End ******* //

{ // ************* PickOption Start ************* //
/***popup:SetLabel*/
/**Set Label*/
Object involved = /** \nObject: *//***tag:object*//**/item/**/;
string labelname = /** \nLabel: *//***tag:label*//**/"ToSwap"/**/;
Variant value = /** \nValue: *//***tag:value*//**/1/**/;

involved.labels.assert(labelname).value = value;
} // ******* PickOption End ******* //

{ // ************* PickOption Start ************* //
/***popup:SetObjectColor*/
/**Set Object Color*/
Object object = /** \nObject: *//***tag:object*//**/item/**/;
object.color = /** \nColor: *//***tag:color*/ /**/Color.byNumber(item.Type)/**/;
} // ******* PickOption End ******* //

{ // ************* PickOption Start ************* //
/***popup:SetLabel*/
/**Set Label*/
Object involved = /** \nObject: *//***tag:object*//**/item/**/;
string labelname = /** \nLabel: *//***tag:label*//**/"Capacity"/**/;
```

```
Array vetttipo = Table.query("SELECT ARRAY_AGG(Type) FROM TypeTable")[1][1];
Array vettcap = Table.query("SELECT ARRAY_AGG(Capacity) FROM TypeTable")[1][1];

for (int i=1; i<= numType; i++){
              if (item.Type == vetttipo[i])
                     involved.labels.assert(labelname).value = vettcap[i];
}
} // ******* PickOption End ******* //

{ // ************* PickOption Start ************* //
/***popup:SetName*/
/**Set Name*/
treenode involved = /** \nObject: *//***tag:object*//**/item/**/;
string name = /** \nName: *//***tag:name*//**/"Battery " +
string.fromNum(nameBattery+1)/**/;

involved.name = name;
nameBattery++;
} // ******* PickOption End ******* //
{ // ************* PickOption Start ************* //
/***popup:SetLabel*/
/**Set Label*/
Object involved = /** \nObject: *//***tag:object*//**/item/**/;
string labelname = /** \nLabel: *//***tag:label*//**/"State"/**/;
Variant value = /** \nValue: *//***tag:value*//**/1/**/;

involved.labels.assert(labelname).value = value;
} // ******* PickOption End ******* //
{ // ************* PickOption Start ************* //
/***popup:SetLabel*/
/**Set Label*/
Object involved = /** \nObject: *//***tag:object*//**/item/**/;
string labelname = /** \nLabel: *//***tag:label*//**/"MaxSoCTime"/**/;
Variant value = /** \nValue: *//***tag:value*//**/-1/**/;

involved.labels.assert(labelname).value = value;
       } // ******* PickOption End ******* //
```

The code reported below [29] is inserted on the On-Entry Trigger of the sink block. It has the purpose of collecting the key performance indicators of the simulations and storing them in the tables.

```
/**Custom Code*/
Object current = ownerobject(c);
Object item = param(1);
int port = param(2);

Object obj = model().find("SwapBay");
obj.labels.assert("Busy").value = 0;

Table table = Table("BatteryTable");
Table table1 = Table("CustomersTable");
int riga = current.labels["Exit"].value;

// update CustomersTable
table1.addRow(riga);
```

```
table1.setRowHeader(riga,"Customer " + string.fromNum(numCustomer));
table1.cell(riga,1).value = item.StartWait;
table1.cell(riga,2).value = item.EndWait;
table1.cell(riga,3).value = item.StartService;
table1.cell(riga,4).value = item.EndService;
table1.cell(riga,5).value = item.EndWait-item.StartWait;
table1.cell(riga,6).value = item.EndService-item.StartService;
table1.cell(riga,7).value = table1.cell(riga,5).value + table1.cell(riga,6).value;

numCustomer++;

// Update BatteryTable
table.addRow(riga);
table.setRowHeader(riga,"Battery " + string.fromNum(numBattery));
table.cell(riga,1).value = item.Type;
table.cell(riga,2).value = item.Capacity;
table.cell(riga,3).value = item.StoringSoC;
table.cell(riga,4).value = item.SoC;
table.cell(riga,5).value = item.EntryTime;
table.cell(riga,6).value = item.MaxSoCTime;
table.cell(riga,7).value = item.OutTime;
table.cell(riga,8).value = item.State;
table.cell(riga,9).value = item.Energy;
table.cell(riga,10).value = item.OutTime-item.EntryTime;

if (item.MaxSoCTime != -1){
	table.cell(riga,11).value = item.OutTime-item.MaxSoCTime;
	table.cell(riga,12).value = item.MaxSoCTime-item.EntryTime;
}
else{
	table.cell(riga,11).value = 0;
	table.cell(riga,12).value = item.OutTime-item.EntryTime;
}

numBattery++;
current.labels.assert("Exit").value+= 1;

//string trackedvar1 = "TimeInSystem1";
//double initial = 0;
//double val = Model.time - getcreationtime(item);
//if (item.Type == 1)
//	TrackedVariable(trackedvar1).value = initial + val;

//string trackedvar2 = "TimeInSystem2";
//double initial2 = 0;
//double val2 = Model.time - getcreationtime(item);
//if (item.Type == 2)
//TrackedVariable(trackedvar2).value = initial2 + val2;
```

The On Model Reset code demonstrated below [29] is executed before the simulations are started in order to assign the capacities of the batteries located in the warehouse and the power values of the charging racks. In addition to that, it is also used to insert the starting values of the parameters into the tables.

```
/* Reset Code */
```

```
Object obj = model().find("BatteryWarehouse");

// Reset TypeTable
Table table = Table("TypeTable");
table.clear();
table.setColHeader(1, "Type");
table.setColHeader(2, "Capacity");
table.setSize(numType, 2);
int tip = 1;
int cap = 198;

for (int i=1; i<=numType; i++){
	table.cell(i,1).value = tip;
	table.cell(i,2).value = cap;
	tip++;
	cap+=66;
}

// Reset BatteryTable
Table table1 = Table("BatteryTable");
table1.clear();
table1.setSize(0,12);
table1.setColHeader(1, "Type");
table1.setColHeader(2, "Capacity");
table1.setColHeader(3, "StoringSoC");
table1.setColHeader(4, "SoC");
table1.setColHeader(5, "EntryTime");
table1.setColHeader(6, "MaxSoCTime");
table1.setColHeader(7, "OutTime");
table1.setColHeader(8, "State");
table1.setColHeader(9, "Energy");
table1.setColHeader(10, "StayTime");
table1.setColHeader(11, "StayTimeToMax");
table1.setColHeader(12, "ChargingTime");

// Reset CustomersTable
Table table0 = Table("CustomersTable");
table0.clear();
table0.setSize(0,7);
table0.setColHeader(1, "StartWait");
table0.setColHeader(2, "EndWait");
table0.setColHeader(3, "StartService");
table0.setColHeader(4, "EndService");
table0.setColHeader(5, "TimeOfWait");
table0.setColHeader(6, "TimeOfService");
table0.setColHeader(7, "TimeInStation");

// Reset WaitTable & PowerTable
Table table2 = Table("WaitTable");
Table table3 = Table("PowerTable");
table2.clear();
int bay = rackgetnrofbays(obj);
int level = rackgetnroflevels(obj);
table2.setSize(level,bay);
table3.setSize(level,bay);

int dimension1 = 1;
for (int i=1; i<=level; i++){
	table2.setRowHeader(i, "Level " + string.fromNum(dimension1));
	table3.setRowHeader(i, "Level " + string.fromNum(dimension1));
	dimension1++;
}

int dimension2 = 1;
for (int i=1; i<=bay; i++){
	table2.setColHeader(i, "Bay " + string.fromNum(dimension2));
```

```
        table3.setColHeader(i, "Bay " + string.fromNum(dimension2));
        dimension2++;
}

for (int i=1; i<=level; i++){
        for (int j=1; j<=bay; j++){
                table2.cell(i,j).value = 0;
                table3.cell(i,j).value = 150;
        }
        }
```

The code reported below [29] is used to raise the SoC level of the battery packs once they have been placed into charging racks. The update rate of the SoC level is determined considering the charging formula stated in Chapter 1 section 1.3 and the maximum charging power. Additionally, the code specifies how much energy is supplied by chargers to each battery packs and calculates the total energy use of the station.

```
/**Custom Code*/
//treenode tree = model().find("BatteryWarehouse");
//Object obj = tree;
//int dimensionrack = obj.subnodes.length;
//return rackgetcellcontent(obj,1,1);

Object obj = model().find("BatteryWarehouse");
int dimensionrack = obj.subnodes.length;
Table table = Table("WaitTable");

Array captot = Array (dimensionrack);
Array charge = Array (dimensionrack);
Array carica = Array (dimensionrack);
Array tempori = Array (dimensionrack);
Array bay = Array(dimensionrack);
Array level = Array(dimensionrack);
double sum = 0;

for (int i=1; i <= dimensionrack; i++){
        captot [i] = obj.subnodes[i].labels["Capacity"].value;
        charge [i] = obj.subnodes[i].labels["StoringSoC"].value;
        tempori [i] = obj.subnodes[i].labels["EntryTime"].value;
        carica [i] = obj.subnodes[i].labels["SoC"].value;
}
// function that returns the new SoC values based on the power supplied by the
charger
Array finale = NewSoC(captot, charge, tempori, carica).clone();

//
update all SoCs in racks
for (int i=1; i <= dimensionrack; i++){
        obj.subnodes[i].labels.assert("SoC").value = finale[i];
        bay [i] = rackgetbayofitem(obj, obj.subnodes[i]);
        level [i] = rackgetlevelofitem(obj, obj.subnodes[i]);
        if (obj.subnodes[i].labels["SoC"].value == MaxLevelRackSoC && tempori[i] != 0
&& table[level[i]][bay[i]] == 0){
                obj.subnodes[i].labels.assert("State").value = 0;
                obj.subnodes[i].labels.assert("MaxSoCTime").value = time();
```

```
                table[level[i]][bay[i]]++;
                }
        sum += obj.subnodes[i].labels.assert("Energy").value;
}
        TotEnergy = sum;
        /**Custom Code*/

/* Custom Code*/
 // totalcapacity -> param(1);
// storingSoC -> param(2);
// timeofentry -> param(3);
// newSoC -> param(4);

Object obj = model().find("BatteryWarehouse");
int dimensionrack = obj.subnodes.length;
Array age = Array (dimensionrack);
Array per = Array (dimensionrack);
Array tocharge = Array (dimensionrack);
Array bay = Array(dimensionrack);
Array level = Array(dimensionrack);
for (int i=1; i <= dimensionrack; i++){
        if (param(4)[i] < MaxLevelRackSoC){
                age [i] = time() - param(3)[i];
                bay [i] = rackgetbayofitem(obj, obj.subnodes[i]);
                level [i] = rackgetlevelofitem(obj, obj.subnodes[i]);
                per [i]= (param(1)[i] -
(age[i]/3600)*Table("PowerTable")[level[i]][bay[i]])/param(1)[i];
                obj.subnodes[i].labels.assert("Energy").value =
Table("PowerTable")[level[i]][bay[i]]*age[i]/3600;
                tocharge [i] = 1 - per[i];
                param(4)[i] = param(2)[i] + tocharge[i]*100;}
        else
        param(4)[i] = MaxLevelRackSoC;
} return param(4);
```

The last code [29] that has been implemented in the model is illustrated below. It enables the station to deal with more than one AGV that may handle multiple workstations. The code controls the movement of AGVs so that the collisions between vehicles and deadlocks in the station are prevented.

```
// Sending logic Object item = param(1);
Object current = ownerobject(c);
/**Shortest Queue if Available*/
/**Send to the port corresponding to the shortest queue downstream that is
available.*/
Object bay1 = model().find("SwapBay");
Object bay2 = model().find("SwapBay2");
Object bay3 = model().find("SwapBay3");
int occupied1 = bay1.labels["Busy"].value;
int occupied2 = bay2.labels["Busy"].value;
int occupied3 = bay3.labels["Busy"].value;
treenode tempobject; int curmincontent = 1000000000;

// this sets the integer to the largest possible value that an integer can hold
double curminindex = 0;
```

```
if ((occupied1 == 1 && occupied2 == 1 && occupied3 == 1) || (occupied1 == 0 &&
occupied2 == 0 && occupied3 == 0))
{ for (int index = 1; index <= current.outObjects.length; index++)

{ // numofoutport tempobject = current.outObjects[index];
// obj connected to the outport=index

if (opavailable(current,index) && tempobject.subnodes.length < curmincontent)
 { curmincontent = tempobject.subnodes.length; curminindex = index; } } return
curminindex;

  // outputport }
   if (occupied1 == 1 && occupied2 == 0 && occupied3 == 0)
    // 1,0,0 return duniform(2,3); // random queue if (occupied1 == 0 && occupied2
== 1 && occupied3 == 0) { // 0,1,0
int count = duniform(1,2);// random queue
if (count == 1){ return 1; } if (count == 2){ return 3; } }
if (occupied1 == 0 && occupied2 == 0 && occupied3 == 1) // 0,0,1
return duniform(1,2); // random queue
if (occupied1 == 1 && occupied2 == 1 && occupied3 == 0) // 1,1,0
return 3;
if (occupied1 == 0 && occupied2 == 1 && occupied3 == 1) // 0,1,1
return 1;
if (occupied1 == 1 && occupied2 == 0 && occupied3 == 1) // 1,0,1
return 2;
```

3.4 Plan of Experiments

The thesis proposes an alternative approach for public transportation in the city of Turin. The transportation services will be carried out by means of electric buses that will be operated under the battery swapping method and the depleted batteries will be replaced with the charged ones by the battery swapping station in which the exhausted batteries will be charged for later use. To put the mentioned scenario in practice, once the hourly arrival rates of the average number of electric buses have been obtained and the simulation models have been created, a series of simulations will be performed to discover: ‘the ideal battery capacity of each station’, ‘the optimal number of stations required in the city of Turin’, and ‘the most convenient configuration of the stations’.

In this section, a plan has been created to identify which scenarios will be simulated to obtain the feasibility assessment and the performance measures of the stations. The experimental plan will be split into two sections. In the first section, the simulation plan will involve a

preliminary analysis to understand the optimal battery capacity for the following cases: 2BSSs, 3BSSs, 4BSSs.

It must be underlined that varying the number of stations has a great influence on the arrival rates. Therefore, the warehouse capacity of each case must be decided in conformity with the arriving rates. Another important parameter that must be taken into account when deciding the optimal battery pack capacity is the provided mean SoC level. Since the stations must provide the batteries with a certain SoC level (80%), the number of battery packs in the warehouse directly affects the SoC level of the provided batteries. Increasing the number of the battery packs located in the warehouse gives an opportunity to the arriving battery packs enough time to charge more and the simulation plan will aim to find the minimum number of battery packs that keep the provided mean SoC level as close as possible to 80%. Consequently, several simulations with varying the number of battery packs have been planned to find the optimal number of battery packs that the warehouse should hold for each case (2BSSs, 3BSSs, 4BSSs) as is reported in Table 3.5.

No. of Experiment	**No. of Battery Packs in the Warehouse**	**Arrival Rates**	**No. of Workstations**	**No. of AGVs Used**	**Average State of Charge (SoC)**
1……20	30……50	Winter-2BSSs	1	1	25%
21……41	30……50	Winter-3BSSs	1	1	25%
41….61	20……40	Winter-4BSSs	1	1	25%

Table 3.5 Experimental plan to find the optimal number of battery packs for 2BSSs, 3BSSs, 4BSSs

In the second part of the experimental plan, after finding the optimal sizing of the warehouse for each case and using these optimal numbers, the simulation plan will involve the

experiments to determine the optimal number of the stations in the Turin and to identify which configuration of the stations reveals the best performance. By varying the number of swapping platforms (battery swap workstations), the size of the AGV fleet used and the arrival rate of the battery packs depending on the number of BSSs, 18 unique scenarios have been obtained and reported in Table 3.6.

No. of Experiment	Arrival Rates	No. of Workstations	No. of AGV	Expected State of Charge
1	Winter-2BSSs	1	1	25%
2	Winter-2BSSs	2	1	25%
3	Winter-2BSSs	2	2	25%
4	Winter-2BSSs	3	1	25%
5	Winter-2BSSs	3	2	25%
6	Winter-2BSSs	3	3	25%
7	Winter-3BSSs	1	1	25%
8	Winter-3BSSs	2	1	25%
9	Winter-3BSSs	2	2	25%
10	Winter-3BSSs	3	1	25%
11	Winter-3BSSs	3	2	25%
12	Winter-3BSSs	3	3	25%
13	Winter-4BSSs	1	1	25%
14	Winter-4BSSs	2	1	25%
15	Winter-4BSSs	2	2	25%
16	Winter-4BSSs	3	1	25%
17	Winter-4BSSs	3	2	25%
18	Winter-4BSSs	3	3	25%

Table 3.5 Planned simulations to find the optimal number of stations and the best performing configuration

4 Simulation Results and Discussion

4.1 Optimization of Number of Battery Packs

Figures 4.1, 4.2, 4.3 demonstrate the relevance between the battery pack capacity and the mean SoC percentage of the batteries provided to the customers. It can be observed that increasing the number of battery packs in the warehouse leads the customer to receive batteries with a higher SoC level. After computing their optimal numbers that result in target SoC (80%), they have been used for the rest of the simulations: 49 for 2BSSs, 44 for 3BSSs, and 35 for 4BSSs.

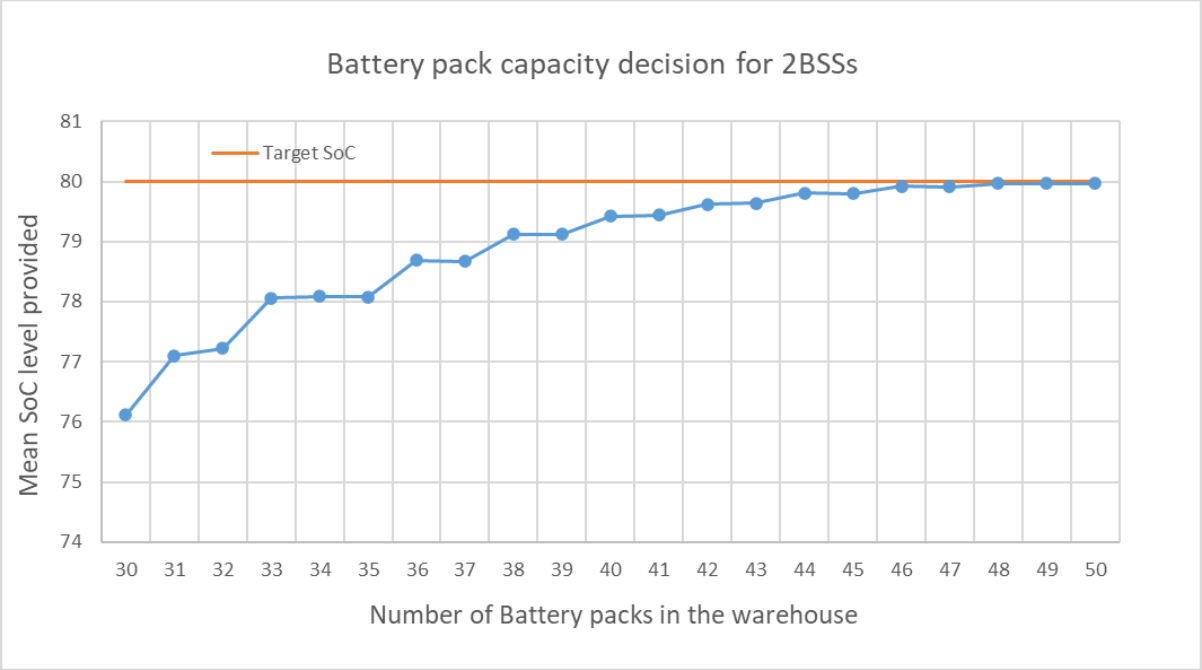

Figure 4.1: Battery Pack Capacity decision for 2BSSs

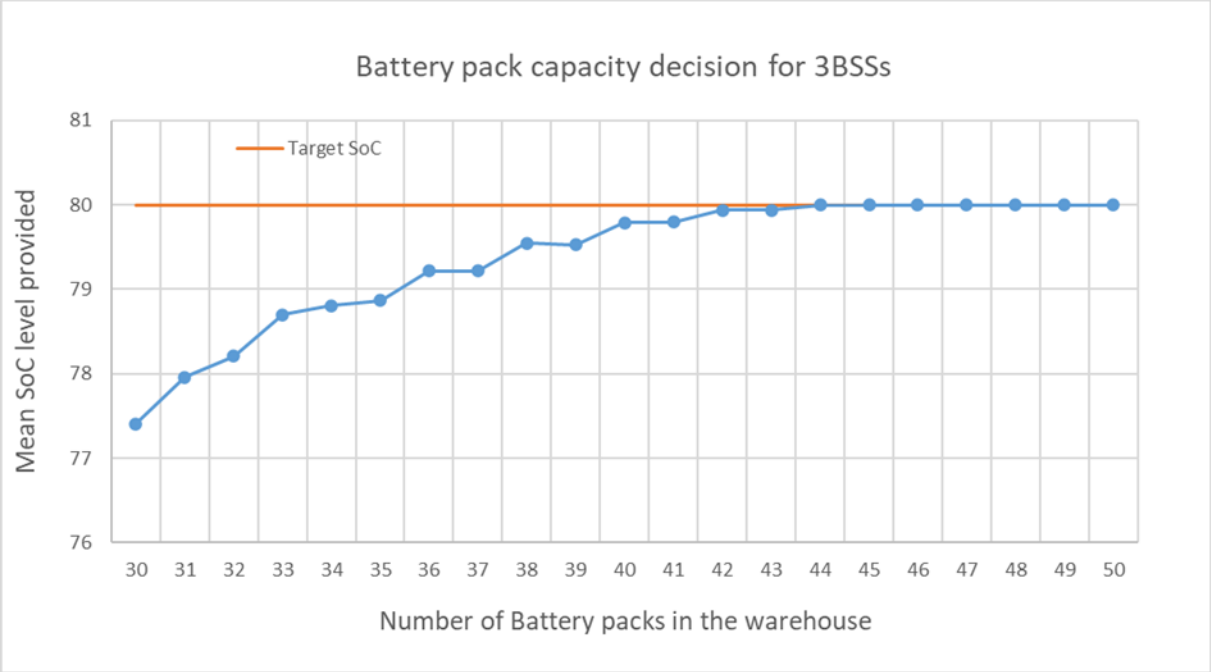

Figure 4.2: Battery Pack Capacity decision for 3BSSs

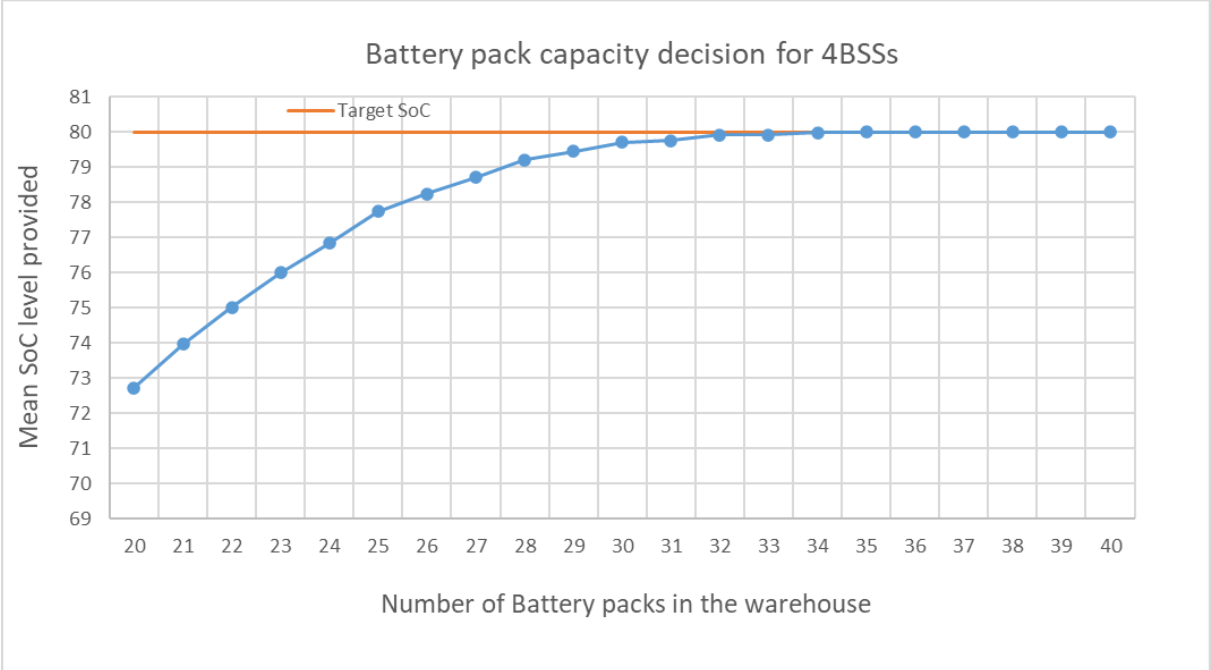

Figure 4.3: Battery Pack Capacity decision for 4BSSs

4.2 SoC of the provided batteries

In Figure 4.4, the mean values of the SoC percentage of the batteries provided to customers for each case have been reported. It is important to realize that the target SoC percentage has been reached by almost all the cases and even the minimum value of 79.45 % is highly reasonable and serviceable.

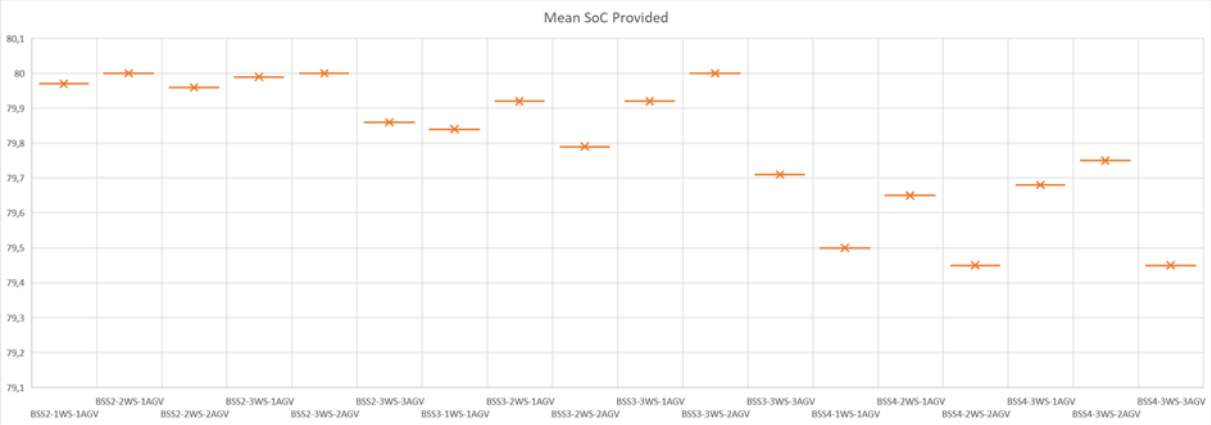

Figure 4.4: SoC of the provided batteries

4.3 Mean Charging Time

With regard to the SoC of the provided batteries which exhibit almost constant value of 80%, it is not surprising to observe the same steady behavior in the mean charging time plot. The figure indicates that every station provides enough time to charge battery packs from 25% to 80%.

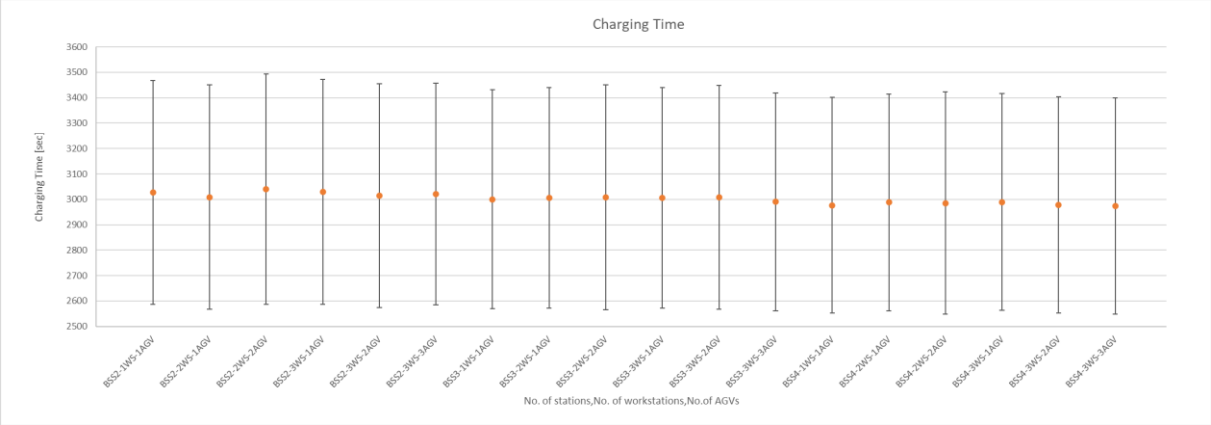

Figure 4.5: Mean Charging Time

4.4 Stay time of fully charged batteries in the rack

Figure 4.4 illustrates the dwell time of fully charged batteries in the rack. Cases with 3 BSSs deliver the highest performance so that the charged batteries have been maintained at the warehouse in a short period of time.

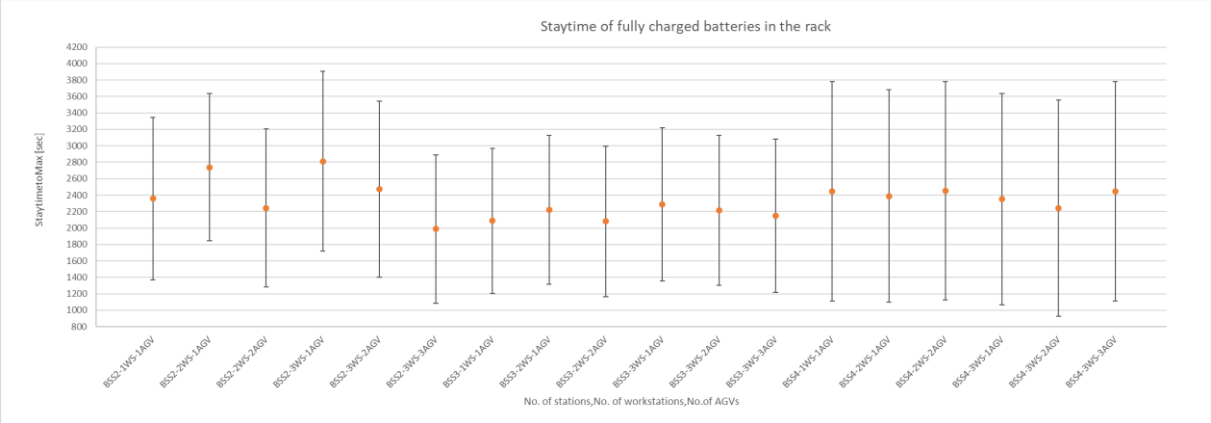

Figure 4.6: Staytime of fully charged batteries in the rack

4.5 Mean Waiting Time

The mean waiting time is one of the most important key performance parameters that must be addressed carefully since it has extreme importance to ensure the continuity of the public transportation. It can be easily verified that increasing the number of BSS (decreasing the arrival rates) shortens the customer's waiting time significantly. Additionally, the cases in which the number of AGVs is equal to the number of workstations enjoy the reduced waiting times compared to others. On the other hand, the least performing cases are the ones that a single AGV is operated for more than one workstation.

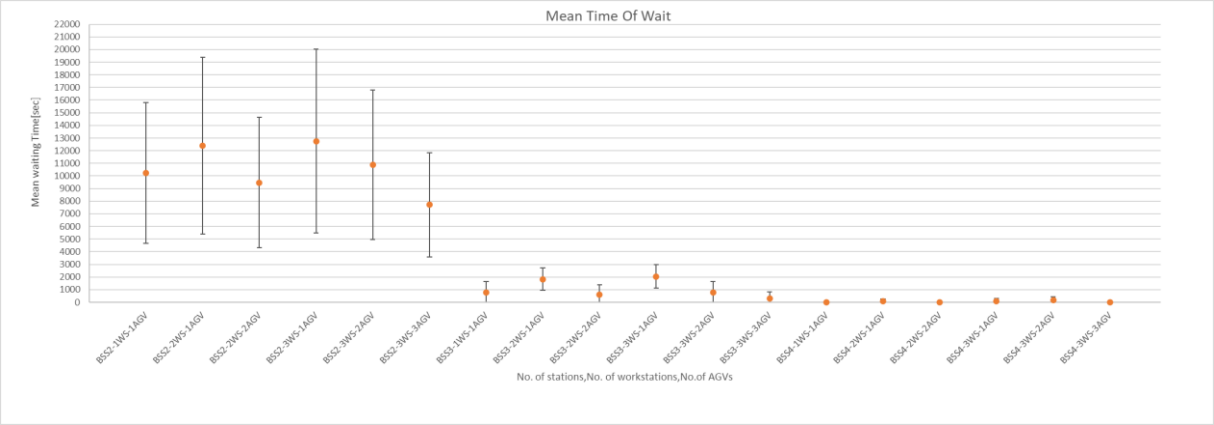

Figure 4.7: Mean Waiting Time

4.6 Mean Service time

A similar trend as in the case of mean waiting time can be detected in the mean service time plot in which equating the number of workstations with the number of AGV is the best way to shorten the mean service time. In addition to that, the cases where the swapping is performed with only one workstation and one AGV reveals the best service performance.

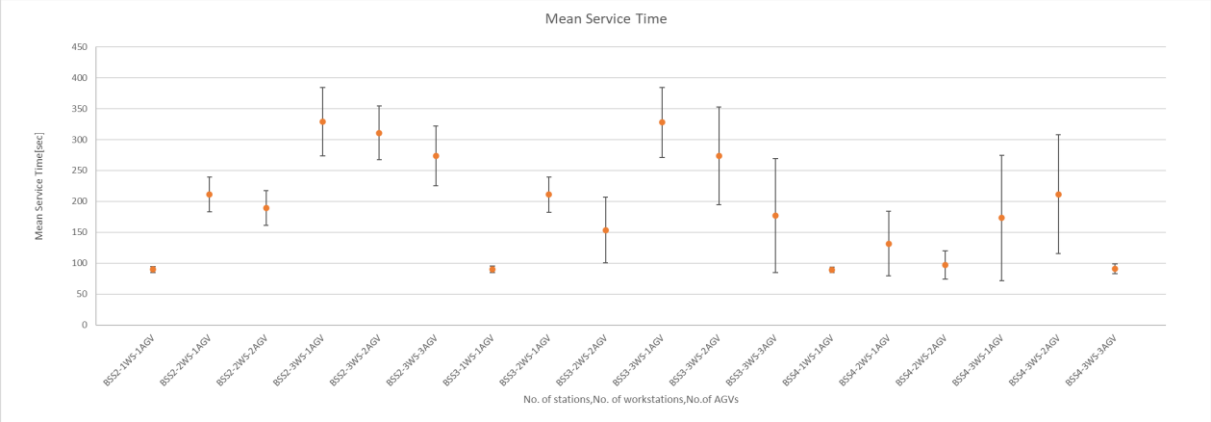

Figure 4.8: Mean Service Time

4.7 Total Energy Consumption

Figure 4.9 shows the energy consumption of each case. The cases of 4BSSs require less energy absorption compared to the other two cases (2BSSs and 3BSSs) as a result of a fewer number of battery packs in the warehouse and decreased arrival rates which give rise to the necessity of charging fewer batteries.

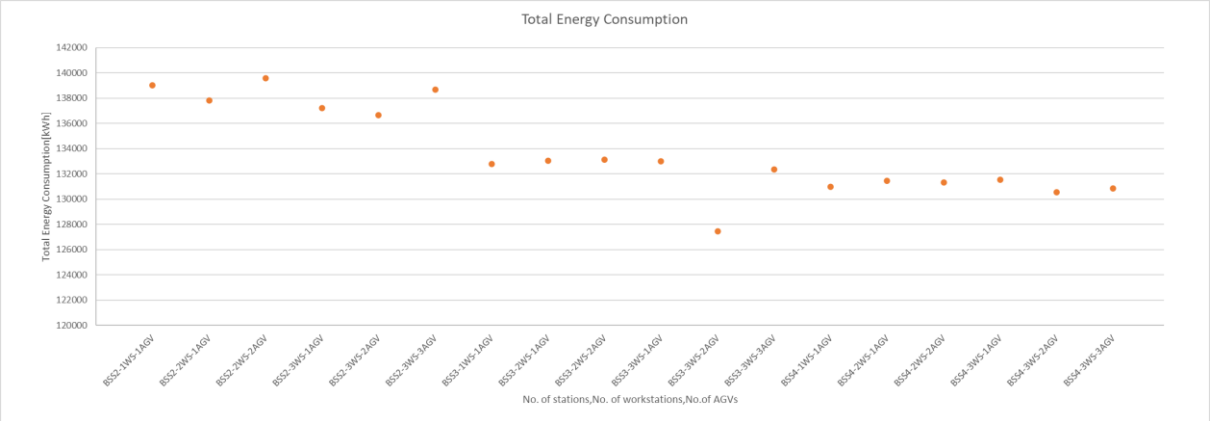

Figure 4.9: Total Energy Consumption

4.8 Vehicles Utilization

The AGV utilization rises when the number of workstations is greater than the number of AGV and its utilization drops significantly if three AGVs are used for three workstations. With regard to ASRS utilization, its value varies with respect to arrival rates. Consequently, since 2 BSSs reveal higher arrival rates, the ASRS utilization reaches its maximum value there.

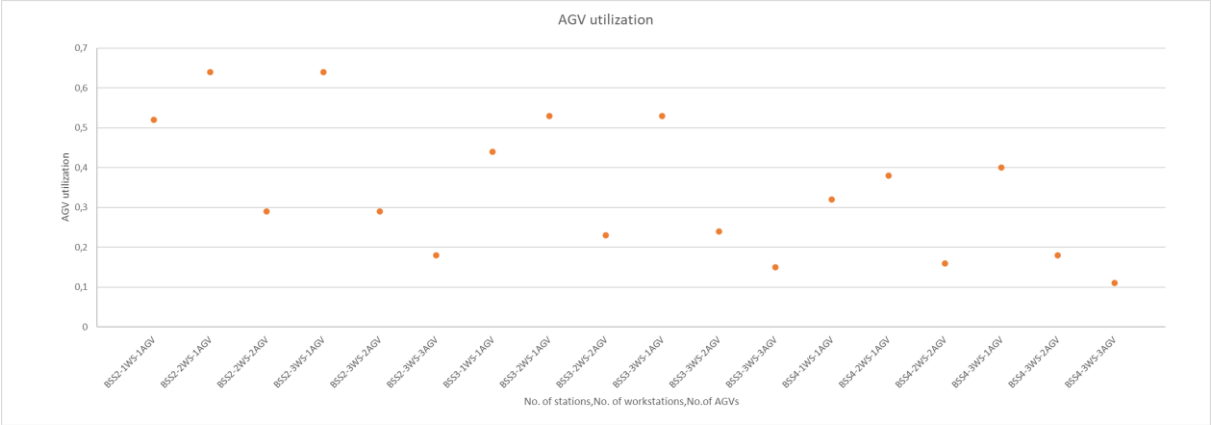

Figure 4.10: AGV Utilization

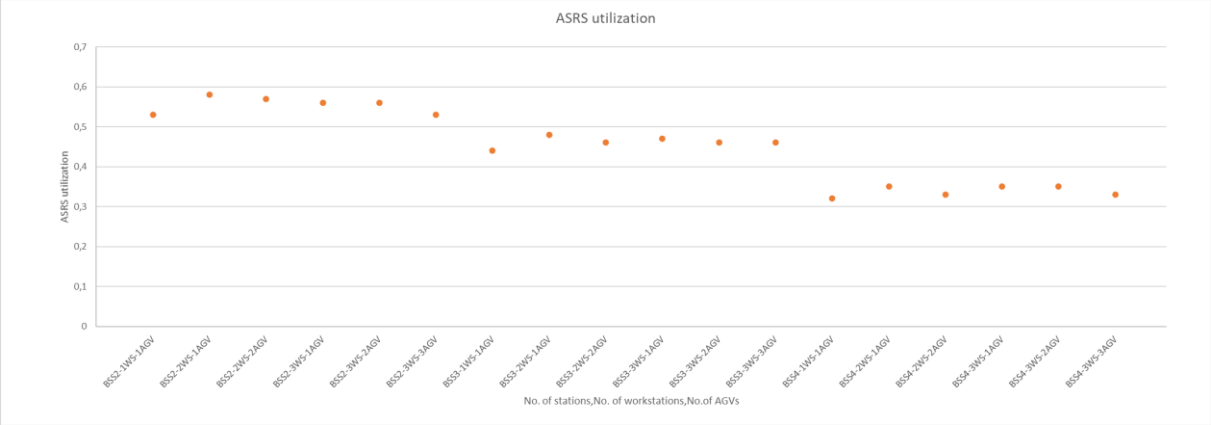

Figure 4.11: ASRS Utilization

4.9 Optimal Configuration Decision

After the simulations have been executed and their results have been obtained, this section is intended to identify the best configuration out of all 18 alternatives that are characterized by multiple conflicting criteria. For this purpose, multi-criteria decision making (MCDM) or also called multiple criteria decision analysis (MCDA) will be performed to compare the performances of the different alternatives and evaluate the optimal scenario. MCDA techniques are powerful methods utilizing computational and mathematical tools with the purpose of enabling the decision-makers to determine the best feasible option among various scenarios. Unlike the traditional single objective decision making whose area of interest is limited by either maximization or minimization of a specific criterion, MCDA methods are capable of analyzing the complex systems that are characterized by several criteria or objectives as in the case of the battery swapping stations. In this regard, different MCDA methods can be implemented to address the issue of the conflicting criteria and eventually find the optimal alternative [30-32]. The general decision-making process can be summarized as follows.

- Designing a system and identifying its objectives.
- Establishing alternative systems.
- Constructing a set of criteria having influences on the systems depending on the objectives.
- Assigning weights/priorities to each criterion based on its importance for the system's objectives.
- Selecting the best fitting MCDA method to the designated systems.
- Application of the chosen MCDA method to evaluate all the alternatives.
- Ranking/prioritizing the alternatives in a subjective reference order according to assigned weights of criteria.
- Determining the best compromise alternative

One can find various MCDA methods in the scientific literature. Weighted Sum Model by Fishburn in 1967, Weighted Product Model by Bridgman 1922, ELECTRE by Benayoun et al. 1966, TOPSIS by Hwang and Yoon 1981, MAUT by Edwards and Newman 1982, PROMETHEE by Brans and Vincke 1985, VIKOR by Opricovic 1998, AHP by Saaty 1970 are some of the most adopted methods by researchers and practitioners in the field of decision making.[30] . Accurate selection of the method is essential since they considerably differ in many aspects including the area of the application, data aggregation method, the methods to determine the preferences and evaluation criteria, implication of uncertainty on the analysis [33]. It has been decided to apply the VIKOR (VlseKriterijuska OptimizacijaI Komoromisno Resenje) as a decision-making method for the evaluation of the optimal BSS scenario since it offers the solution for the discrete decision-making problems that contain non-commensurable (different units) and incompatible(conflict) criteria while seeking to achieve enhanced group utility of the majority(maximum group utility) and limited individual regret of the opponent[31-34]. VIKOR method, standing for multi-criteria optimization and compromise solution, was firstly introduced by Serafim Opricovic in 1990. The method forms the multiple criteria ranking index using an aggregating function which is responsible to measure the closeness of each alternative to the ideal solution and rank a set of alternatives according to each criterion function. Therefore, in this method, without showing any biased towards any alternatives, decision-makers look for the compromise solution which is the closest to the ideal solution and that one is considered as feasible one [31-36]. Figure 4.12 demonstrates the flow chart of the VIKOR method, and it represents the method's structure with the brief explanation and sequence of each step in the diagram.

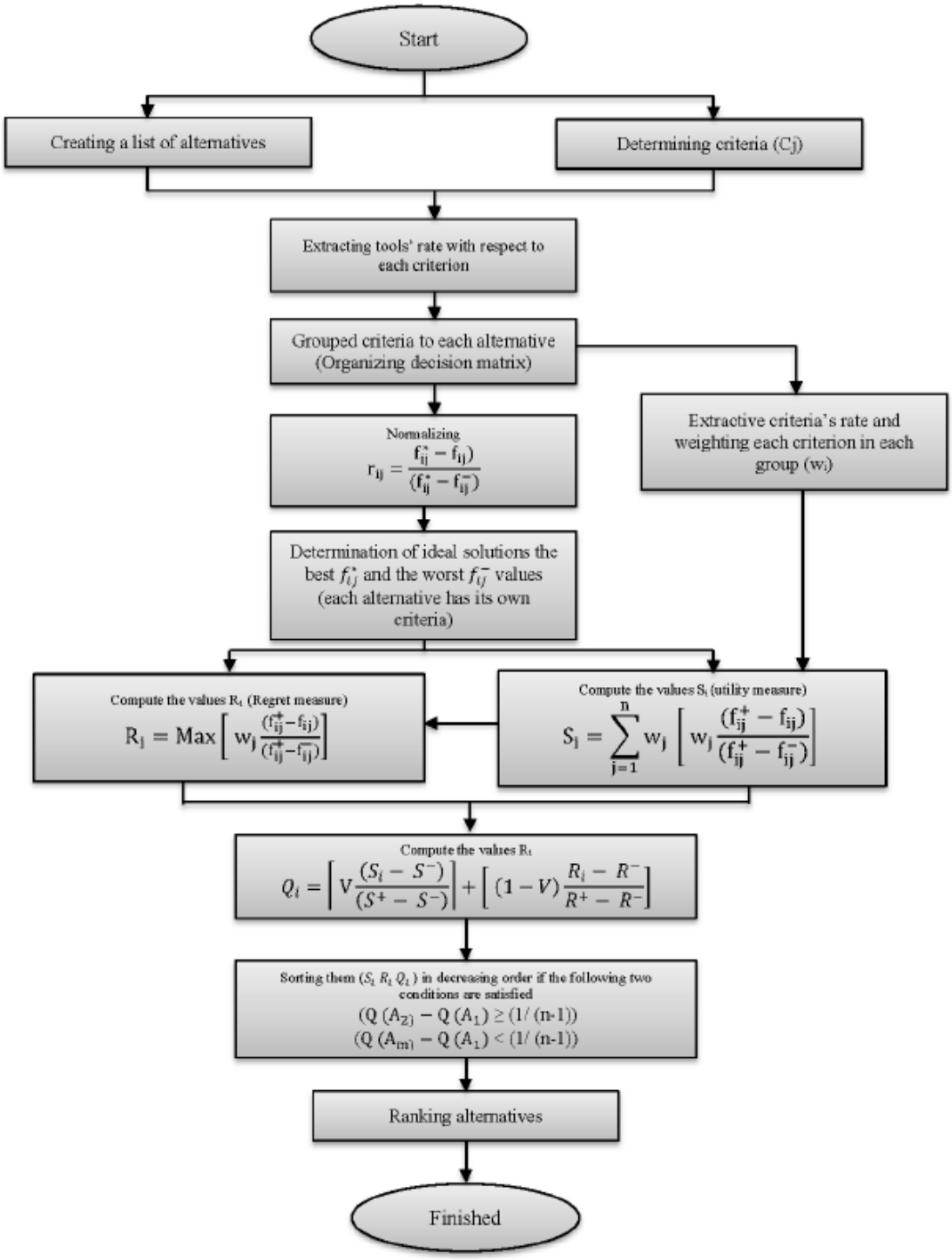

Figure 4.12: Diagram of adopted VlseKriterijuska Optimizacija Komoromisno Resenje (VIKOR) technique[37]

Step 1: A variety of alternatives are denoted as A_1, A_2,…A_i,…A_m where m is the number of alternatives and it is equal to 18.

Alternatives			
A_1	BSS2-1WS-1AGV	**A_{10}**	BSS3-3WS-1AGV
A_2	BSS2-2WS-1AGV	**A_{11}**	BSS3-3WS-2AGV
A_3	BSS2-2WS-2AGV	**A_{12}**	BSS3-3WS-3AGV
A_4	BSS2-3WS-1AGV	**A_{13}**	BSS4-1WS-1AGV
A_5	BSS2-3WS-2AGV	**A_{14}**	BSS4-2WS-1AGV
A_6	BSS2-3WS-3AGV	**A_{15}**	BSS4-2WS-2AGV
A_7	BSS3-1WS-1AGV	**A_{16}**	BSS4-3WS-1AGV
A_8	BSS3-2WS-1AGV	**A_{17}**	BSS4-3WS-2AGV
A_9	BSS3-2WS-2AGV	**A_{18}**	BSS4-3WS-3AGV

Table 4.1: All 18 alternatives evaluated

Step 2: For alternative A_i, the rating of the jth criterion is denoted by f_{ij}, i.e. f_{ij} is the rating (key performance score) of the jth criterion function for the alternative A_i, where n is the number of criteria and it is equal to 8.

Alternatives	Mean Time Of Wait	Mean Time Of Service	Mean SoC	Total Energy Consumption	Mean StayTime To Max	Number of Workstation	Total Number of Battery Packs	Number of AGVs
A_1	10246,99	90,06	79,97	139027,04	2356,896476	1	98	2
A_2	12402,09	211,18	80	137793,42	2737,561851	2	98	2
A_3	9469,33	189,35	79,96	139555	2244,405773	2	98	4
A_4	12757,23	328,78	79,99	137200,86	2812,728018	3	98	2
A_5	10883,4	310,72	80	136664,5	2472,513499	3	98	4
A_6	7708,32	273,62	79,86	138681,32	1989,37081	3	98	6
A_7	761,53	89,92	79,84	132764,01	2086,168918	1	132	3
A_8	1825,79	210,97	79,92	133017,72	2221,643977	2	132	3
A_9	591,62	153,74	79,79	133133,58	2080,128534	2	132	6
A_{10}	2039,71	327,73	79,92	133009,26	2286,540745	3	132	3
A_{11}	763,86	273,62	80	127442,04	2213,702183	3	132	6
A_{12}	308,77	177,15	79,71	132338,01	2147,525045	3	132	9
A_{13}	13,96	89,44	79,5	130960,76	2443,639547	1	140	4
A_{14}	88,81	131,63	79,65	131454,68	2388,704204	2	140	4
A_{15}	0	97,25	79,45	131324	2453,04332	2	140	8
A_{16}	92,54	173,31	79,68	131535,08	2350,379234	3	140	4
A_{17}	167,94	211,63	79,75	130536,04	2240,925992	3	140	8
A_{18}	0	90,96	79,45	130824,72	2445,541399	3	140	12

Table 4.2: Performance scores of each alternative with respect to each criterion

Step 3: W_j is the weight of the jth criterion (weight coefficients associated to the different criteria), stating the relative importance of the criteria, where j =1, 2,…,n; and $W_j \in [0,1]$, $W_1+W_2+\ldots+W_n=1$.

Criterion Name	Criterion	Weight	Weight Coefficent
Mean Time Of Wait	f_1	W_1	0,4
Mean Time Of Service	f_2	W_2	0,15
Mean SoC	f_3	W_3	0,025
Total Energy Consumption	f_4	W_4	0,25
Mean StayTime To Max	f_5	W_5	0,025
Number of Workstation	f_6	W_6	0,05
Number of Battery Packs	f_8	W_8	0,05
Number of Vehicles	f_9	W_9	0,05

Table 4.3: Weight coefficients associated to the different criteria

Step 4: Identify the best fj* and the worst fj− values of all given criterion functions, j=1,2,…,n; If the criteria demand the minimum values(cost function), the best value is the lowest one and the highest one is the worst and on contrary, if the criteria request the maximum value(benefit function), the best value is the highest one and the worst value is the lowest one.

$$f_j^* = \max_i f_{ij}, \quad f_j^- = \min_i f_{ij}$$

Criterion	f_1	f_2	f_3	f_4	f_5	f_6	f_8	f_9
fj*	0	89,44	80	127442	1989,37081	1	98	2
fj-	12757,23	328,78	79,45	139555	2812,728018	3	140	12

Table 4.4: The best and the worst values of all criterion functions

Step 5: Calculate the values of S_i and R_i using the formulas reported below where S_i denotes the utility measure whereas R_i stands for the regret measure; i =1, 2,. . ., m. S_i measures the relative distance between alternative, '' i '' and the positive ideal solution (also called the best combination or expected solution) and R_i refers to the regret of the alternative '' i '' (also called the most uncomfortable option or pessimistic solution) and indicates the relative distance from the positive ideal solution.

$$S_i = \sum_{j=1}^{n} w_j (f_j^* - f_{ij}) / (f_j^* - f_j^-),$$
$$R_i = \max_j w_j (f_j^* - f_{ij}) / (f_j^* - f_j^-),$$

	f_1	f_2	f_3	f_4	f_5	f_6	f_8	f_9	S_i	R_i
A_1	0,321292	0,000389	0,001364	0,239103	0,011159	0	0	0	0,573307	0,321292
A_2	0,388865	0,076297	0	0,213643	0,022718	0,025	0	0	0,726522	0,388865
A_3	0,296909	0,062616	0,001818	0,25	0,007744	0,025	0	0,01	0,654087	0,296909
A_4	0,4	0,15	0,000455	0,201413	0,025	0,05	0	0	0,826867	0,4
A_5	0,341246	0,138681	0	0,190343	0,01467	0,05	0	0,01	0,744941	0,341246
A_6	0,241693	0,11543	0,006364	0,231968	0	0,05	0	0,02	0,665454	0,241693
A_7	0,023878	0,000301	0,007273	0,10984	0,002939	0	0,040476	0,005	0,189707	0,10984
A_8	0,057247	0,076166	0,003636	0,115077	0,007053	0,025	0,040476	0,005	0,329655	0,115077
A_9	0,01855	0,040298	0,009545	0,117468	0,002756	0,025	0,040476	0,02	0,274094	0,117468
A_{10}	0,063955	0,149342	0,003636	0,114902	0,009023	0,05	0,040476	0,005	0,436334	0,149342
A_{11}	0,023951	0,11543	0	0	0,006811	0,05	0,040476	0,02	0,256668	0,11543
A_{12}	0,009681	0,05497	0,013182	0,101048	0,004802	0,05	0,040476	0,035	0,30916	0,101048
A_{13}	0,000438	0	0,022727	0,072623	0,013793	0	0,05	0,01	0,169581	0,072623
A_{14}	0,002785	0,026441	0,015909	0,082817	0,012125	0,025	0,05	0,01	0,225077	0,082817
A_{15}	0	0,004895	0,025	0,08012	0,014079	0,025	0,05	0,03	0,229093	0,08012
A_{16}	0,002902	0,052563	0,014545	0,084476	0,010961	0,05	0,05	0,01	0,275448	0,084476
A_{17}	0,005266	0,076579	0,011364	0,063857	0,007638	0,05	0,05	0,03	0,294704	0,076579
A_{18}	0	0,000953	0,025	0,069815	0,013851	0,05	0,05	0,05	0,259619	0,069815

Table 4.5: Computation of the utility and regret measures

Step 6: Calculate the values Q_i; i = 1,2,. . .,m, by the formula reported below. The formula includes the variable v as the weight for the strategy of maximum group utility (majority criteria) and 1-v as the weight of the individual regret. When v>0.5, the decision-maker tends to emphasize the maximum group utility (majority agreement), and when v<0.5, the results will be based on majority negative attitude. Therefore, here it is assumed v=0.5.

$$Q_i = v(S_i - S^*)/(S^- - S^*) + (1 - v)(R_i - R^*)/(R^- - R^*)$$

where

$$S^* = \min_i S_i, \quad S^- = \max_i S_i,$$
$$R^* = \min_i R_i, \quad R^- = \max_i R_i,$$

$(S_i - S^-) / (S^* - S^-)$ Closeness to ideal solution

$(S_i - R^-) / (R^* - R^-)$ Closeness to anti-ideal solution

	Si	Ri	Qi
A_1	0,573307	0,321292	0,687928
A_2	0,726522	0,388865	0,906805
A_3	0,654087	0,296909	0,712453
A_4	0,826867	0,4	1
A_5	0,744941	0,341246	0,848707
A_6	0,665454	0,241693	0,637487
A_7	0,189707	0,10984	0,07592
A_8	0,329655	0,115077	0,190308
A_9	0,274094	0,117468	0,151664
A_{10}	0,436334	0,149342	0,323348
A_{11}	0,256668	0,11543	0,135322
A_{12}	0,30916	0,101048	0,153474
A_{13}	0,169581	0,072623	0,004252
A_{14}	0,225077	0,082817	0,061905
A_{15}	0,229093	0,08012	0,060876
A_{16}	0,275448	0,084476	0,102735
A_{17}	0,294704	0,076579	0,105424
A_{18}	0,259619	0,069815	0,068492
S*,R*	0,169581	0,069815	
S-,R-	0,826867	0,4	

Table 4.6: Computation of ranking values

Step 7: Alternatives are ranked according to the values of Si, Ri, and Qi in decreasing order and the alternative A' which is ranked first by the Q measure can be decided as the best alternative if the following two conditions are fulfilled:

- Condition 1-Acceptable advantage: $Q(A_2) - Q(A_1) \geq (1/(n-1))$ where A_1 and A_2 are the first and second alternatives in the Q ranking list; n is the number of alternatives
- Condition 2-Acceptable stability in decision making: The alternative A_1 must also be ranked in the first position by Si or/and Ri.

If both conditions are not satisfied, a set of compromise alternatives is suggested as follows.

- If only Condition 2 is not satisfied, A_1 and A_2 are the best alternatives.
- If Condition 1 is not satisfied, A_1, A_2,....., A_m are the best alternatives, and A_m is decided by the following relation $Q(A_m) - Q(A_1) \leq (1/(n-1))$.

Alternatives	Rank based on Si	Rank based on Ri	Rank based on Qi
A_1	13	15	14
A_2	16	17	17
A_3	14	14	15
A_4	18	18	18
A_5	17	16	16
A_6	15	13	13
A_7	2	8	5
A_8	11	9	11
A_9	7	11	9
A_{10}	12	12	12
A_{11}	5	10	8
A_{12}	10	7	10
A_{13}	1	2	1
A_{14}	3	5	3
A_{15}	4	4	2
A_{16}	8	6	6
A_{17}	9	3	7
A_{18}	6	1	4

Table 4.7: Ranking of the alternatives

- Condition 1: Q (A_2)- Q (A_1) = 0,056624 ≤ 0,058823529 =(1/(n-1)). The equation shows that Condition 1 is not satisfied.
- Condition 2: Since the alternative A_{13} ranked best by Qi is also ranked best by Si, Condition 2 is fully satisfied.

Due to the fact that one of the conditions is not satisfied, the VIKOR model proposes a set of compromise solutions. It suggests that if Condition 1 is not satisfied then A_1, A_2,….., A_m are the best alternatives, and A_m is decided by the following relation Q (A_m)-Q (A_1) ≤(1/(n-1). The alternative satisfying the inequality has been found and it is the alternative A_3 (Q (A_3)-Q (A_1) = 0,05765304≤0,058823529=(1/(n-1).)

Consequently, the alternatives A_{13}, A_{15}, and A_{14} have been found as the best alternatives and they correspond to 4Stations-1AGV-1Workstation, 4Stations-2AGVs-2Workstations, and 4 Stations-1AGV-2Workstations.

4.10 Cost Analysis of the Optimal Configuration

This section estimates the initial investments required to introduce the electric-powered buses operating under the battery swapping method to the public transportation system of Turin and it will analyze specifically the cost perspective of the optimal cases that have been discovered in Section 4.9. The purchase cost of the battery-electric buses is the most critical cost item that must be addressed carefully since it counts the major part of the up-front investments. The acquisition cost of BEBs is significantly greater than the other public transit alternatives and it is almost twice as the cost of regular diesel buses which varies in the range of 220 thousand and 380 thousand EUR [38-40]. However, one may find variable purchase costs of the BEBs in the literature and the global market depending on the dissimilar regional market conditions and the procurement processes which adopt different discount rates [41]. The report of Forbes [42] and Bloomberg [43] present the average price of 12-meter electric buses by leaving aside the battery cost and it has been reported as 440,000 €. Therefore, in the analysis, the unit price is set as 440,000 € and the battery cost will be added on it to obtain the total purchase cost of BEB. A recent report [44], 'Electric Vehicle Outlook 2020' was published by Bloomberg to draw attention to the latest developments on the battery technology and their impacts on the battery prices. It states that the volume-weighted price of lithium-ion battery packs has reached $156/kWh on average, falling 87% from 2010 to 2019 and this downtrend is expected to continue as a consequence of the development of the new chemistries, advanced manufacturing techniques, and innovative pack designs. Another report [45], Global EV Outlook 2019, released by IEA presents more representative data about the battery price of electric buses, stating that the electric buses travelling 40,000-50,000 km/year display an average battery price around 216 € /kWh and hence it has been decided to apply this quantity for the cost analysis. Charging equipment of the BSS is another significant cost item that has been estimated for the cost analysis. The researches have been conducted by ICTT [46] and EvGO [47] with the purpose of estimating the charging equipment costs. The researches provide the price of the chargers that varies with respect to the charging level (Level1, Level 2, and DC fast), and the power of the chargers. The model assumes the

charging of the battery packs with DC fast charging that provides maximum charging power of 150 kW and the acquisition cost of these chargers has been reported as 62.250€/unit in the analysis of the above-mentioned papers. The last cost items are the internal logistic vehicles, i.e. AGV and ASRS. The unit price of them has been found in the [48] and [49] respectively. The average cost of AGV can range between 83.000€ and 125.000 € meanwhile, the average cost of ASRS (Mini-Load ASRS) is around 1.666.000€. Table 4.8 provides the estimation of the required initial investment by breaking down each cost item that is essential for the operation of the BSS.

Cost Items	**Unit Price**	**Number of the Item**	**Cost of the Items**
Battery Electric Buses	440.000 €/bus	416	183.040.000€
198 kWh Battery Packs for BEB	216 € /kWh	416 x 53%=221	198x216x221=9.451.728€
264 kWh Battery Packs for BEB	216 € /kWh	416 x 47%=195	264x216x195=11.119.680€
198 kWh Battery Packs for 4BSSs	216 € /kWh	35x4x53%=74	198x216x74=3.164.832€
264 kWh Battery Packs for 4BSSs	216 € /kWh	35x4x47%=66	264x216x66=3.763.584€
DC fast chargers with power of 150 kW	62.250 €/charger	35x4=140	62.250x140=8.715.000 €
AGV	83.000€/AGV	2x4=8	83.000x8=664.000 €
ASRS	1.666.000€/ASRS	1x4=4	4x1.666.000€=6.664.000 €
Total Cost of the Optimal Alternative			226.582.824 €

Table 4.8: Estimated cost of the optimal alternative

5 Conclusion and Future Work

In this paper, battery swapping technology has been introduced as a novel method to manage the public transportation system and the city of Turin has been selected as a case study. The swapping demand of the BEB fleets or in other words, the arriving schedule of the electric buses to BSSs has been found out through the simulation model developed in Anylogic software which predicts the arriving times by simulating the trip of each bus considering the route lengths, battery pack capacities, and energy consumptions. Then, the station has been modelled by using the Flexsim software and several simulations have been executed by varying the number and the configuration of the station in order to obtain the best alternatives. There are three main contributions of the thesis which can be used as a design guide for the governments, municipal corporations, and bus companies which have intentions to invest in this subject. Firstly, it provides sizing(capacity) analysis of the BSSs by specifying the number of battery packs that must be hold by each station. Secondly, it proposes a feasibility and performance analysis to determine how many stations must be in service in Turin and which station configuration is the best fitting case in terms of performance. Lastly, to estimate the initial investment required for the best alternative, a cost analysis has been presented by stating each cost item in the station and their corresponding prices. Furthermore, there are still some future concepts and research areas that can be implemented to improve the established model of designated swapping stations:

- The model assumes the charging of the battery packs via energy taken from the electricity grid. Consequently, this may originate a negative impact on the electricity distribution network e.g. overloading to the power grid especially in peak hours. To reduce the excessive charging loads on the grid, the station model can be also extended with the installation of the renewable energy infrastructure as a second source for charging.

- The ‘Parallel Swapping Technique’, the removal of the depleted batteries and the installation of the charged batteries carried out simultaneously, can be adopted so that the further reduction in the service time is accomplishable.
- To come up with more accurate data on the arrival schedule of the stations, the relevant electric buses can be experimented on the public road under real-world traffic conditions with the pilot infrastructure of the BSSs.
- Implementing the possible maintenance and breakdown events on the simulation model to check the influence on the performance and continuity of the operations.
- The model can be enhanced by advanced codes that monitor continuously the degradation level (Loss of efficiency) of each battery pack and estimate the remaining lifespan of the batteries after each charging and discharging cycle.

Abbreviations

(MCDA) Multiple-Criteria Decision Analysis

(OEM) Original Equipment Manufacturer

(EV) Electric Vehicle

(SoC) State of Charge

(BSS) Battery Swapping Station

(FIFO) First in First Out

(SOH) State of Health

(IEC) International Electro Technical Commission

(SAE) Society of Automotive Engineers

(CCS) Combined Charging System

(GIS) Geographic Information System

(AGV) Automated Guided Vehicle

(AGRS) Automated Storage and Retrieval System

(MCDM) Multi-Criteria Decision Making

(BEB) Battery Electric Bus

References

[1] Ritchie, H., & Roser, M. “Emissions by sector”. Our World in Data. Retrieved from https://ourworldindata.org/emissions-by-sector.

[2] “Electric Bus Market Outlook and Projections, Worldwide, 2019-2027”. (2020, January 10). Retrieved from https://www.prnewswire.com/news-releases/electric-bus-market-outlook-and-projections-worldwide-2019-2027-300984888.html.

[3] “Electric Bus Market.”. Market Research Firm. Retrieved from https://www.marketsandmarkets.com/Market-Reports/electric-bus-market-38730372.html

[4] “Electric Bus Market: Growth, Statistics, Industry Forecast 2019-2024.” Electric Bus Market. Retrieved from https://www.mordorintelligence.com/industry-reports/automotive-electric-bus-market.

“ELECTRIC BUS MARKET (2020-2025)”. (Rep.). (2019). Mordor Intelligence.

[5] Adnane Houbbadi, Serge Pelissier, Rochdi Trigui, Eduardo Redondo-Iglesias,Tanguy Bouton. (2019, May). “Overview of Electric Buses deployment and its challenges related to the charging-the case study of TRANSDEV”. 32nd Electric Vehicle Symposium (EVS32). LYON, France.11p.hal-02148377v2.

[6] Ou, S., Lin, Z., Wu, Z., Zheng, J., Lyu, R., Przesmitzki, S. V., & He, X. (2017, January). “A Study of China s Explosive Growth in the Plug-in Electric Vehicle Market”. Oak Ridge National Laboratory.doi:10.2172/1341568. ORNL/TM-2016/750.

[7] Prescient & Strategic Intelligence Private Limited. (2020, March 19). “Global EV Battery Swapping Market is Driven by Low Penetration of DC Fast Charging Station and Remunerative Prospects for Shared E-Mobility Services: P&S Intelligence”. Retrieved from www.globenewswire.com/news-release/2020/03/19/2003424/0/en/Global-EV-Battery-Swapping-Market-is-Driven-by-Low-Penetration-of-DC-Fast-Charging-Station-and-Remunerative-Prospects-for-Shared-E-Mobility-Services-P-S-Intelligence.html#:~:text=Swapping%20technology%20drastically%20decreases%20the

[8] Adegbohun, F., Jouanne, A. V., & Lee, K. (2019, February 19). “Autonomous Battery Swapping System and Methodologies of Electric Vehicles”. Energies, vol.12, no 4, p.667. doi:10.3390/en12040667

[9] Ahmad, F., Alam, M. S., Alsaidan, I. S., & Shariff, S. M. (2020, April 15). “Battery swapping station for electric vehicles: Opportunities and challenges”. IET Smart Grid, 3(3), 280-286. doi:10.1049/iet-stg.2019.0059

[10] Iclodean, C., Varga, B., Burnete, N., Cimerdean, D., & Jurchiş, B. (2017, October). “Comparison of Different Battery Types for Electric Vehicles”. IOP Conference Series: Materials Science and Engineering, vol 252, p.012058. doi:10.1088/1757-899x/252/1/012058

[11] Falvo, M. C., Sbordone, D., Bayram, I. S., & Devetsikiotis, M. (2014). “EV charging stations and modes: International standards. 2014 International Symposium on Power Electronics, Electrical Drives, Automation and Motion”. doi:10.1109/speedam.2014.6872107

[12] Dericioğlu, Ç, Yirik, E., Ünal, E., Cuma, M. U., Onur, B., & Tümay, M. (2018). “A Review of Charging Technologies for Commercial Electric Vehicles. International Journal of Advances on Automotive and Technology”. doi:10.15659/ijaat.18.01.892

[13] Ayob, A., Mahmood, W. M., Mohamed, A., Wanik, M. Z., Siam, M. M., Sulaiman, S., . . . Ali, M. A. (2014, January 10). “Review on Electric Vehicle, Battery Charger, Charging Station and Standards”. Research Journal of Applied Sciences, Engineering and Technology. vol 7, no 2, pp. 364-373. doi:10.19026/rjaset.7.263

[14] “How Long Does It Take to Charge an Electric Car?”. (2020, May 28). Retrieved from https://pod-point.com/guides/driver/how-long-to-charge-an-electric-car

[15] “What Determines the Charge Speed?”. (2021, December). Retrieved from https://support.fastned.nl/hc/en-gb/articles/205694717-What-determines-the-charge-speed-

[16] “BU-1003a: Battery Aging in an Electric Vehicle (EV).” Retrieved from https://batteryuniversity.com/learn/article/bu_1003a_battery_aging_in_an_electric_vehicle_ev

[17] Sears, J., Roberts, D., & Glitman, K. (2014). “A comparison of electric vehicle Level 1 and Level 2 charging efficiency”. 2014 IEEE Conference on Technologies for Sustainability (SusTech). Portland. pp 255-258, doi:10.1109/sustech.2014.7046253

[18] Genovese, A., Ortenzi, F. Villante, C. (2015, December). “On the Energy Efficiency of Quick DC Vehicle Battery Charging.”. World Electric Vehicle Journal, vol. 7, no. 4, 1 Dec. 2015, pp. 570–576, www.mdpi.com/2032-6653/7/4/570, 10.3390/wevj7040570

[19] Inventors: Jun Seok Park, Seoul (KR); Won-Kyu (58) Field of Classification Search Kim, Seoul (KR); Hee-Jeing Park, USPC Gunpo-si (KR); Hee Seok Moon, Asan-si (KR); Woongchul Choi, Seoul (KR); Jayil Jeong, Seoul (KR); Chi Man Yu, Bucheon-si (KR); Do Yang Jung. Anyang-si (KR); Yong-hark Shin, Seoul (KR); Jae-Hong Park, Seoul (KR) (73). “BATTERY EXCHANGING METHOD FOR (52) U.S. Cl.”. Patent No.: US 8,963,495 B2. Assignee: Kookmin University Industry Academy Cooperation Foundation, Seoul (KR)

[20] Inventors: Jun Seok Park, Seoul (KR); Won-Kyu Kim, Seoul (KR); Hee-Jeing Park, Gunpo-si (KR); Hee Seok Moon, Asan-si (KR); Woongchul Choi, Seoul (KR); Jayil Jeong, Seoul (KR); Chi Man Yu, Bucheon-si (KR); Do Yang Jung. Anyang-si (KR); Yong-hark Shin,Seoul (KR); Jae-Hong Park, Seoul (KR) (73).” BATTERY EXCHANGING-TYPE CHARGING STATION SYSTEM FOR ELECTRIC VEHICLE (75).”. Patent No.: US 9,156,360 B2. Assignee: KOOKMIN UNIVERSITY INDUSTRY ACADEMY COOPERATION FOUNDATION, Seoul (KR).

[21] Applicants: Kookmin University Industry Academy Cooperation Foundation, Seoul (KR); Industry-University Cooperation Foundation of Korea Aerospace University, Goyang-si, Gyeonggi-do (KR) Jun Seok Park, Seoul (KR); Won-Kyu Kim, Seoul (KR); Won-Jae Jung, Chuncheon-si (KR).” BATTERY EXCHANGE SYSTEM ELECTRIC BUS AND ELECTRIC BUS.”. Patent No.: US 9,026,357 B2. Assignees: Kookmin University Industry Academy Cooperation Foundation, Seoul (KR); Industry-University Cooperation Foundation of Korea Aerospace University,

[22] Kim, J., Song, I., & Choi, W. (2015, July 7). “An Electric Bus with a Battery Exchange System. Energies”. vol. 8, no.7. pp6806-6819. doi:10.3390/en8076806.

[23] Li, W., Li, Y., Deng, H., & Bao, L. (2018, July 18). “Planning of Electric Public Transport System under Battery Swap Mode”. Sustainability, vol. 10 no. 7, p.2528. doi:10.3390/su10072528

[24] Moon, J., Kim, Y. J., Cheong, T., & Song, S. H. (2020, February 5). “Locating Battery Swapping Stations for a Smart e-Bus System”. Sustainability, vol.12, no.3, p.1142. doi:10.3390/su12031142

[25] Adnane Houbbadi, Serge Pelissier, Rochdi Trigui, Eduardo Redondo-Iglesias,Tanguy Bouton. (2019, May). “Overview of Electric Buses deployment and its challenges related to the charging-the case study of TRANSDEV”. 32nd Electric Vehicle Symposium (EVS32). LYON, France.11p.hal-02148377v2.

[26] Krawiec, S., Karoń, G., Janecki, R., Sierpiński, G., Krawiec, K., & Markusik, S. (2016). “Economic Conditions to Introduce the Battery Drive to Busses in the Urban Public Transport”. Transportation Research Procedia, vol. 14, pp.2630-2639. doi:10.1016/j.trpro.2016.05.420

[27] “GTT LINEE URBANE E SUBURBANE”.. Retrieved from http://www.gtt.to.it/cms/percorari/urbano?view=linee&bacino=U

[28] “Electric bus energy consumption in ViriCiti's spotlight. A report.” (2020, July 28). Sustainable Bus. Retrieved from https://www.sustainable-bus.com/news/electric-bus-consumption-energy-report-viriciti/

“ViriCiti Report E-BUS PERFORMANCE”. (Rep.). (2020, March). VIRICITI

[29] Stefano Locardo.,(2019). “Design and Simulation of an Innovative System of Battery Swapping for Electric Vehicles”.

[30] Kumar, A., Sah, B., Singh, A. R., Deng, Y., He, X., Kumar, P., & Bansal, R. (2017, March). “A review of multi criteria decision making (MCDM) towards sustainable renewable energy development”. Renewable and Sustainable Energy Reviews, vol.69, pp.596-609. doi:10.1016/j.rser.2016.11.191.

[31] Anvari, A., Zulkifli, N., & Arghish, O. (2013, December 12). “Application of a modified VIKOR method for decision-making problems in lean tool selection”. The International Journal of Advanced Manufacturing Technology, vol.71 no.5-8, pp. 829-841. doi:10.1007/s00170-013-5520-x.

[32] Yazdani, M., & Graeml, F. R. (2014, April). “VIKOR and its Applications”. International Journal of Strategic Decision Sciences, vol.5 no.2, pp. 56-83. doi:10.4018/ijsds.2014040105

[33] Wątróbski, J., Jankowski, J., Ziemba, P., Karczmarczyk, A., & Zioło, M. (2019, February). “Generalised framework for multi-criteria method selection: Rule set database and exemplary decision support system implementation blueprints”. Data in Brief, vol. 22, pp. 639-642. doi:10.1016/j.dib.2018.12.015

[34] Sayadi, M. K., Heydari, M., & Shahanaghi, K. (2009, May). “Extension of VIKOR method for decision making problem with interval numbers”. Applied Mathematical Modelling, vol.33 no.5, pp.2257-2262. doi:10.1016/j.apm.2008.06.002

[35] Zimonjić,S. Đekić,.M, Kastratović,E. “APPLICATION OF VIKOR METHOD IN RANKING THE INVESTMENT PROJECTS”. Faculty for Business Economics and Entrepreneurship, Belgrade, Srbija.

[36] Acuña-Soto, C. M., Liern, V., & Pérez-Gladish, B. (2019, February 11). “A VIKOR-based approach for the ranking of mathematical instructional videos”. Management Decision, vol. 57 no.2, pp. 501-522. doi:10.1108/md-03-2018-0242

[37] Mardani, A., Zavadskas, E., Govindan, K., Senin, A. A., & Jusoh, A. (2016,January 4). “VIKOR Technique: A Systematic Review of the State of the Art Literature on Methodologies and Applications”. Sustainability, vol.8 no.1, p.37. doi:10.3390/su8010037

[38] Victor Hug. “Copenhagen trial with 12 m B.Y.D K9 electric buses”. (Rep.). (2015, September 1). Movia

[39] Laizāns, A., Graurs, I., Rubenis, A., & Utehin, G. (2016). “Economic Viability of Electric Public Busses: Regional Perspective”. Procedia Engineering, vol.134, pp.316-321. doi:10.1016/j.proeng.2016.01.013

[40] “Marketplace, economic, technology, environmental and policy perspectives for fully electric buses in the EU (2018, November.). Transport & Environment. Retrieved from https://www.transportenvironment.org/sites/te/files/publications/Electric buses arrive on time.pdf

[41] Quarles, N., Kockelman, K. M., & Mohamed, M. (2020,May 13). “Costs and Benefits of Electrifying and Automating Bus Transit Fleets”. Sustainability, vol.12 no.10, p.3977. doi:10.3390/su12103977

[42] Blanco, S. (2019, April 19). “Proterra Ready For Electric Bus Battery Leasing With $200-Million Credit Facility”. Forbes.Retrieved from https://www.forbes.com/sites/sebastianblanco/2019/04/18/proterra-ready-for-electric-bus-battery-leasing-with-200-million-credit-facility/

[43] “Electric Buses in Cities Driving towards Cleaner Air and Lower CO 2” - Bloomberg Finance L.P”. Retrieved from https://data.bloomberglp.com/professional/sites/24/2018/05/Electric-Buses-in-Cities-Report-BNEF-C40-Citi.pdf

[44] “BNEF EVO Report 2020: Bloomberg New Energy Finance”. Bloomberg Finance LP. (2020.). Retrieved from https://about.bnef.com/electric-vehicle-outlook/

[45] “Global EV Outlook 2019 – Analysis”.(2019).IEA. Retrieved from https://www.iea.org/reports/global-ev-outlook-2019

[46] Nicholas,M. “Estimating electric vehicle charging infrastructure costs across major U.S. metropolitan areas”.(2019,August) .The International Council on Clean Transportation.

[47] Levy.J, Riu.I, Zoi.C. “The Costs of EV Fast Charging Infrastructure and Economic Benefits to Rapid Scale-Up.”(2020,May 18).EVgo FAST CHARGING.

[48] “How Much Does an AGV System Cost?”. . Retrieved from www.scottautomation.com/news/articles/how-much-does-an-agv-system-cost/#:~:text=By%20some%20accounts%2C%20and%20as

[49] Dube, C. (2021, February 02). “Calculating the Cost of ASRS: 5 Contributing Factors”. Retrieved from https://us.blog.kardex-remstar.com/asrs-cost-factors#:~:text=Starting%20Costs%20of%20an%20(ASRS